Impacts of soil management and climate on saturated and near-saturated hydraulic conductivity: analyses of the Open Tension-disk Infiltrometer Meta-database (OTIM)

Authors

Guillaume Blanchy[1], Lukas Albrecht[2], Gilberto Bragato[3], Sarah Garré[1], Nicholas Jarvis[4], John Koestel[2,4]

[1]*Flanders Research Institute for Agriculture, Fisheries and Food (ILVO), Melle, Belgium*

[2]*Agroscope, Reckenholzstrasse 191, 8046 Zürich, Switzerland*

[3]*Council for Agricultural Research and Economics (CREA), Via Po, 14, 00198 Roma, Italy*

[4]*Department of Soil and Environment, Swedish University of Agricultural Sciences (SLU), P.O. Box 7014, 750 07 Uppsala, Sweden*

Corresponding author

John Koestel (johannes.koestel@agroscope.admin.ch)

Keywords

hydraulic conductivity, saturated hydraulic conductivity Ks, near-saturated hydraulic conductivity, Kunsat, Knearsat, soil hydraulic properties, infiltration, tension-disk infiltrometer, soil properties, climate, soil, agricultural management practice, pedo-climatic factors, meta-analysis

Abstract

Saturated and near-saturated soil hydraulic conductivities K_h (~~mm.h~~mm h^{-1}) determine the partitioning of precipitation into surface runoff and infiltration and are fundamental to soils' susceptibility to preferential flow. Recent studies have found indications that climate factors influence K_h, which is highly relevant in the face of climate change. In this study, we investigated relationships between pedo-climatic factors and K_h and also evaluated effects of land use and soil management. To this end, we collated the Open Tension-disk Infiltrometer Meta-database (OTIM), which contains 1297 individual data entries from 172 different publication sources. We analysed a spectrum of saturated and near-saturated hydraulic conductivities at matric potentials between 0 to 100 mm. We found that methodological details like the direction of the wetting sequence or the choice of method for calculating infiltration rates to hydraulic conductivities had a large impact on the results. We therefore restricted ourselves to a subset of 466 of the 1297 data entries with similar methodological approaches. Correlations between K_s and K_h at higher supply tensions decreased especially close to saturation, indicating a different flow mechanism at and very close to saturation as towards the dry end of the investigated tension range. Climate factors were better correlated to topsoil near-saturated hydraulic conductivities at supply tensions ≥ 30 mm than soil texture, bulk density and organic carbon content. We find it most likely that the climate variables are proxies for soil macropore networks created by respective biological activity, pedogenesis and climate specific land use and management choices. Due to incomplete documentation in the source publications of OTIM, we could investigate only a few land use types and agricultural management practices. Land use, tillage system and soil compaction significantly influenced K_h, with effect sizes appearing comparable to the ones of soil texture and soil organic carbon. The data in OTIM show experimental bias is present, introduced by the choice of measurement time relative to soil tillage, experimental design or data evaluation procedures. The establishment of best-practice rules for tension-disk infiltrometer measurements would therefore be helpful. Future studies are needed to investigate how climate shapes soil macropore networks and how land use and management can be adapted to improve soil hydraulic properties. Both tasks require large amounts of new measurement data with improved documentation on soil biology and land use and management history.

1. Introduction

Climate models predict more frequent extreme weather events such as high intensity rainfall with the onset of global warming. To prevent water runoff and erosion, soils need to be able to conduct sometimes large amounts of water in a short time. It is generally accepted that one key soil property is the saturated hydraulic conductivity K_s (~~mm.h~~mm h^{-1}), as it determines the partitioning of precipitation into surface runoff and infiltration. A large K_s reduces erosion risks and allows water to infiltrate into deeper soil layers, where it may replenish an important reservoir of plant available water or contribute to groundwater recharge. The hydraulic conductivity of a soil decreases with decreasing water content, i.e. with decreasing water saturation. The hydraulic conductivity in the so-called near-saturated range (between 0 and 100 mm matric tensions) is likewise important. For rainfall intensities smaller than but close to K_s, ~~S~~soils with larger near-saturated hydraulic conductivity K_h (~~mm.h~~mm h^{-1}) ~~tend~~ will remain less water-saturated because they are able to conduct the precipitation water in smaller macropores~~to generate less water flow in macropore networks~~. Therefore, they are less susceptible to preferential flow (Larsbo et al., 2014) by which agrochemicals and other solutes quickly leach towards the groundwater. Moreover, a large K_h also indicates a well-aerated soil, which drains faster and helps air to escape the soil in case of heavy rainfall. This further reduces the risk of surface runoff and erosion as entrapped air strongly decreases soil hydraulic conductivity.

Saturated hydraulic conductivity is measured either in the laboratory on small cylinders, usually with diameters < 7 cm (Klute ~~&~~and Dirksen, 1985) or it is acquired from field measurements, either using single or double ring infiltrometer methods (Angulo-Jaramillo et al., 2000). In addition, near-saturated hydraulic conductivities can be measured using a tension disk infiltrometer. The method is designed as a field method, but has been occasionally applied in the laboratory. Using a tension disk infiltrometer, hydraulic conductivities at supply tensions between ca. 0.5 and ca. 60 to 150 mm can be obtained, depending on the specifications of the infiltrometer. All measurement techniques for saturated and near-saturated hydraulic conductivity are laborious, time-consuming and constrained to a relatively small soil volume.

It is necessary to develop pedotransfer functions to estimate soil hydraulic conductivities for large-scale modelling applications, as we cannot measure everywhere (Bouma, 1988; Van Looy et al., 2017; Wösten et al., 2001). The development of a pedotransfer function requires a database from which it can be derived. For example, the well-known pedotransfer function ROSETTA (Schaap et al., 2000) is based on the open UNSODA database (Nemes et al., 2001). The equations published in Tóth et al., 2015 are derived from the proprietary EU-HYDI database (Weynants et al., 2013). The pedotransfer functions of Jarvis et al. (2013) are based on an unpublished meta-database containing tension-disk infiltrometer data. Collecting published measurements of saturated and near-saturated hydraulic conductivity measurements into meta-databases and pairing them with other existing databases is essential to develop pedotransfer functions. A notable example is the SWIG database (Rahmati et al., 2018) that collates more than 5000 datasets from soil infiltration measurements, covering the entire globe. Another big effort in collecting information on saturated hydraulic conductivity is the newly published SoilKsatDB (Gupta et al., 2021a), which combines saturated hydraulic conductivity data from several large databases, amongst others UNSODA and SWIG, together with additional measurements published in independent scientific studies. However, none of the databases cited above provide open-access infiltration measurements at tensions near-saturation (h > 0 mm), which limits their use to the estimation of saturated hydraulic conductivity.

While reasonably good estimations of K_s from easy-to-measure or readily available site properties appear to be possible for peat soils (Morris et al., 2022), ~~P~~pedotransfer functions for ~~saturated hydraulic conductivity~~ K_s of mineral soils exhibit ~~rather~~ poor predictive performance with coefficients of determination R^2 not exceeding 0.25. (Weynants et al., 2009; Jorda et al., 2015). Early approaches, like HYPRES (Wösten et al., 1999) and ROSETTA, focused solely on soil properties like texture, bulk density and organic carbon content as predictors for K_s. At the time, it was not sufficiently recognized that soil K_s is mostly determined by the morphology of macropore networks, especially in finer-textured soils (Vereecken et al., 2010; Koestel et al., 2018; Schlüter et al., 2020). A pedotransfer function for K_s requires therefore ideally a database that contains direct information on the macropore network itself. But since such measures are even more cumbersome and time-consuming to obtain (e.g. by X-ray tomography) than measuring hydraulic conductivity itself, it is more reasonable and makes more sense to use proxies from which the macrostructure in a soil can be inferred. Ideal candidates would be root growth and the activity of soil macrofauna, which both strongly determine the development of macropore networks in soil (Meurer et al., 2020). However, they are difficult to measure. Proxies that are more promising are land use and farming practises, such as tillage or soil compaction due to trafficking. Plant growth and soil macrofauna in turn are influenced by the local climate. The climate also sets boundaries for the land use and the associated soil management practices, and thus provides feedback to root growth and macro-faunal activity. Wetting and drying cycles and thus the formation and closure of cracks also are regulated by the climate as is splash erosion and soil crusting. It is therefore not surprising that climate variables typically are correlated with saturated and near-saturated hydraulic conductivities (Jarvis et al., 2013; Jorda et al., 2015; Hirmas et al., 2018; Gupta et al., 2021b). Jorda et al., 2015 found that land use itself was the most important predictor for saturated hydraulic conductivity.

The time of measurement of the hydraulic conductivity (or soil sampling) also has a crucial impact. In an agricultural soil, the hydraulic properties of a freshly prepared seedbed differ from those measured later at harvest. Several studies have demonstrated the evolution of hydraulic conductivity with time (Messing ~~&~~and Jarvis, 1990; Messing and Jarvis, 1993; Bodner et al., 2013; Sandin et al., 2017). Soil management options (such as tillage or the use of cover crops) actively influence the soil saturated and near-saturated hydraulic conductivity. Information on their impact is therefore especially important, but so far has hardly been investigated in meta-studies.

In this study, we quantified the effect of soil management practices on soil saturated and near-saturated hydraulic conductivity, K_h. We also compared the strengths of relationships between K_h and soil management practices and other potentially important influencing factors like soil properties, local climate and details of the measurement methods. In this process, we expanded and published the previously unpublished meta-database on tension-disk infiltration measurements that was first reported by Jarvis et al. (2013). We referred to this database as OTIM in the following (Open Tension-disk Infiltrometer Meta-Database). It complements the currently available public databases on hydraulic conductivities, which are strongly based on laboratory measurements or ring infiltrometer methods.

2 Material and Methods

2.1 Meta-Database, OTIM

2.1.1 Data collection

The first version of OTIM was compiled for the study by Jarvis et al., 2013. The original database contained 753 tension-disk infiltrometer data entries collated from 124 source publications, covering 144 different locations around the globe. We have extended this database by 544 new tension-disk infiltrometer data entries from 48 additional studies that had been published after 2012. The search for publications was carried out between 2021-05-31 and 2021-06-23 using the queries and search engines detailed in Table A1.

We found 115 publications containing tension-disk infiltrometer measurements published in 2013 or later. We retained the data for further analysis when (i) K_h or the infiltration rate was measured at more than two tensions larger or equal to 5 mm and (ii) sufficient meta-data on soil and site properties (at least soil texture) as well as soil management practices (at least land use and tillage) were available. If a publication only reported infiltration rates, we calculated hydraulic conductivity using the method of Ankeny et al. (1991). Only 45 of the 115 publications fulfilled the above-mentioned criteria. Table A2 summarises how many papers were rejected and for which reasons. For 27 of the 45 retained studies, we digitised the published K_h values from figures using WebPlotDigitizer (open-source web-based software created by Ankit Rohatgi, https://automeris.io/WebPlotDigitizer/). For cases in which K_h measurements were mentioned in a publication, but the results were not reported, we contacted the corresponding authors. We received the data in this fashion for three of these publications (Alletto et al., 2015; Larsbo et al., 2016a; Meshgi ~~&~~and Chui, 2013). The new studies containing data were added to the OTIM database are summarised in Table 1.

Table 1: List of new entries added to the Jarvis et al., 2013 database.

Reference	**Land use**	**Tillage**	**Compaction**	**Sampling time**	**Data entries**
Alagna et al., 2015	grassland	no tillage	not compacted	consolidated soil	1
Alletto et al., 2015	arable	conventional tillage	unknown	consolidated soil	60
Bagarello et al., 2014	arable	no tillage		unknown	unknown	10

		conventional tillage			
Baranian Kabir et al., 2020	grassland | arable	no tillage	not compacted | compacted	unknown | consolidated soil	4
Báťková et al., 2020	arable	reduced tillage | no tillage | conventional tillage	unknown	consolidated soil | soon after tillage	12
Bodner et al., 2013	arable	no tillage	unknown	soon after tillage | consolidated soil	12
Bottinelli et al., 2013	arable	unknown | conventional tillage | reduced tillage | no tillage	unknown	consolidated soil	10
Costa et al., 2015	arable	conventional tillage | reduced tillage | no tillage	not compacted	consolidated soil	3
De Boever et al., 2016	grassland	no tillage	not compacted	unknown	6
Tóth et al., 2014	arable	conventional tillage	not compacted | compacted	consolidated soil	2
Etana et al., 2013	arable	conventional tillage	not compacted | compacted	unknown	2

Fashi et al., 2018	arable	no tillage | reduced tillage | conventional tillage	compacted | not compacted	unknown	8
Fasinmirin et al., 2018	arable | woodland/plantation | grassland	conventional tillage | no tillage	not compacted | compacted	unknown	3
Greenwood, 2016	arable | grassland	conventional tillage | no tillage	unknown	consolidated soil	4
Hallam et al., 2020	arable	conventional tillage	not compacted	unknown	60
Hardie et al., 2012	arable	no tillage	not compacted	consolidated soil	2
Holden et al., 2014	grassland	no tillage	not compacted	consolidated soil	5
Hyväluoma et al., 2019	arable	conventional tillage	unknown	consolidated soil	4
Iovino et al., 2016	arable | grassland | woodland/orchard	reduced tillage | no tillage	unknown	consolidated soil	3
Kelishadi et al., 2013	arable | grassland	reduced tillage | no tillage | conventional tillage	not compacted	consolidated soil	4

Keskinen et al., 2019	arable	no tillage | conventional tillage	unknown	consolidated soil	15
Khetdan et al., 2017	arable	no tillage	unknown	unknown	4
Larsbo et al., 2016a	arable	conventional tillage	not compacted | compacted	consolidated soil | unknown	5
Lopes et al., 2020	woodland/orchard | grassland	no tillage	not compacted	consolidated soil	4
Lozano et al., 2014	arable	no tillage	not compacted	consolidated soil	2
Lozano-Baez et al., 2020	grassland | woodland/orchard	no tillage	not compacted	unknown	18
Matula et al., 2014	grassland	no tillage	unknown	unknown	3
Miller et al., 2018	arable	conventional tillage	unknown	consolidated soil	10
Mirzavand, 2016	arable	conventional tillage | reduced tillage | no tillage	unknown	consolidated soil	12
Pulido Moncada et al., 2014	arable | grassland	conventional tillage | no tillage	unknown	unknown	4

Rahbeh, 2019	arable	conventional tillage	unknown	consolidated soil	69
Rienzner ~~&~~and Gandolfi, 2013	arable	conventional tillage	not compacted	unknown | consolidated soil	18
Sandin et al., 2017	arable	conventional tillage	not compacted | compacted	consolidated soil | unknown	7
Soracco et al., 2015	grassland	conventional tillage	not compacted | compacted	unknown	3
Soracco et al., 2019	arable	conventional tillage | no tillage	unknown	consolidated soil	6
Wang, 2021	arable	conventional tillage	unknown	soon after tillage | consolidated soil	25
Wanniarachchi et al., 2019	arable	conventional tillage	unknown	consolidated soil	6
Yu et al., 2013	grassland	no tillage	unknown	unknown	11
Yusuf et al., 2017	arable	no tillage	not compacted	consolidated soil	1
Yusuf et al., 2020	arable	no tillage	not compacted	consolidated soil	5

Zeng et al., 2013	woodland/orchard	conventional tillage	unknown	consolidated soil	20
Zeng et al., 2012	grassland	no tillage	unknown	consolidated soil	6
Zhang et al., 2013	grassland | arable	no tillage | unknown	unknown	consolidated soil	6
Zhang et al., 2014	arable	conventional tillage	unknown	consolidated soil	4
Zhang et al., 2016	woodland/orchard | arable	no tillage | conventional tillage	unknown | not compacted	consolidated soil | soon after tillage	24
Zhang et al., 2021	grassland | woodland/orchard | arable	no tillage | conventional tillage	unknown	consolidated soil	4
Zhao et al., 2014	arable | grassland	conventional tillage | no tillage	not compacted	unknown	12
Zhou et al., 2015	arable | grassland | woodland/orchard	conventional tillage | no tillage	not compacted	soon after tillage	3

In addition to adding data from new publications to OTIM, we also revisited the studies contained in the original version of the database and collected additional information on soil management practices associated with the measured data. For each soil management option, OTIM contains two columns. In the first column, the information as given in the source publication is stored. The second column summarises this information into a few classes, which were subsequently used in the meta-analysis. In this study, we investigated effects of land use, tillage system, soil compaction and day of measurement relative to the latest tillage operation on the field. A compaction class was assigned to a data entry only if the plot had been described as ‘compacted’ or ‘not compacted’ in the source publication. ‘Compacted’ data entries corresponded, for example, to infiltration measurements in wheel tracks or on plots of a compaction experiment. The day of measurement relative to tillage was also included, with the data labelled ‘freshly tilled’ when the authors in the source publication stated that the measurements had taken place soon after tillage. Otherwise, it was assumed that the soil ~~had~~ already had time to consolidate before the infiltration measurements were carried out. All soil texture data ~~was~~ were mapped onto the USDA classification system using the method proposed in Nemes et al. (2000).

2.1.2. Climate data and soil classification

The climatic data entries provided in the database were created using the bioclimatic raster data (BioClim) provided by WorldClim (worldclim.org). The data was averaged across the years 1970 to 2000 and had a 30 arc second resolution (~1 km^2; Fick ~~&~~and Hijmans, 2017). The available climate variables were mean annual temperature and precipitation, the mean temperature as well as mean precipitation of the warmest, coldest, wettest and driest quarter and month, respectively, the isothermality, the mean diurnal and annual temperature range, the seasonality for temperature and precipitation. Besides the bio-climatic data in WorldClim we included the aridity index (here defined as the annual precipitation divided by the potential evapotranspiration) as well as the average annual potential evapotranspiration (ET$_0$). Both were inferred from the “Global Aridity Index and Potential Evapotranspiration Climate Database v2” that is based on the WorldClim database (Trabucco ~~&~~and Zomer, 2019). The World Reference Base (WRB) soil type was also extracted from the source publications. When it was not reported, the SoilGrids database by ISRIC (Poggio et al., 2021) was used to infer it. The map contained information about the main soil type regarding the WRB classes (IUSS Working Group WRB, 2015). The most probable soil type was chosen for each location. For all discussed climate and soil maps, the python package “rasterio” (v1.2.10) was used to collect the variables from the corresponding raster cell at the location coordinates given in the source publications.

2.1.3 Model fit to infer K_h at near-saturated tensions not measured

Tension-disk infiltrometers measure infiltration rates at a specific supply tension (Angulo-Jaramillo et al., 2000). They consist of a ceramic disk to which a water reservoir and a bubbling tower is attached. The ceramic disk is saturated and hydraulically connected to the soil by inserting a layer of fine sand between the disk and the soil surface. The supply tension at the bottom of the ceramic disk is adjusted by the bubbling tower. The measured unconfined (i.e. three-dimensional) infiltration rates are then commonly converted to hydraulic conductivities with the aid of the Wooding equation (Wooding, 1968). Note that unconfined tension-disk infiltrometers cannot provide measurements at a tension of zero, i.e. K_s. Even if many publications report K_s values obtained from tension-disk infiltrometers, these measurements must have been conducted at tensions slightly larger than zero, as water would otherwise have freely leaked out of the tension disk. For this reason, we set the tensions for K_s measurements to 1 mm, but still referred to these data as saturated hydraulic conductivity. Note that we discuss matrix potentials in terms of tensions (negative pressures) throughout this manuscript. For convenience, we denote K_h at a specific tension by replacing the subscript h by the tension value in mm. For example, K_{100} denotes K_h at a supply tension of 100 mm.

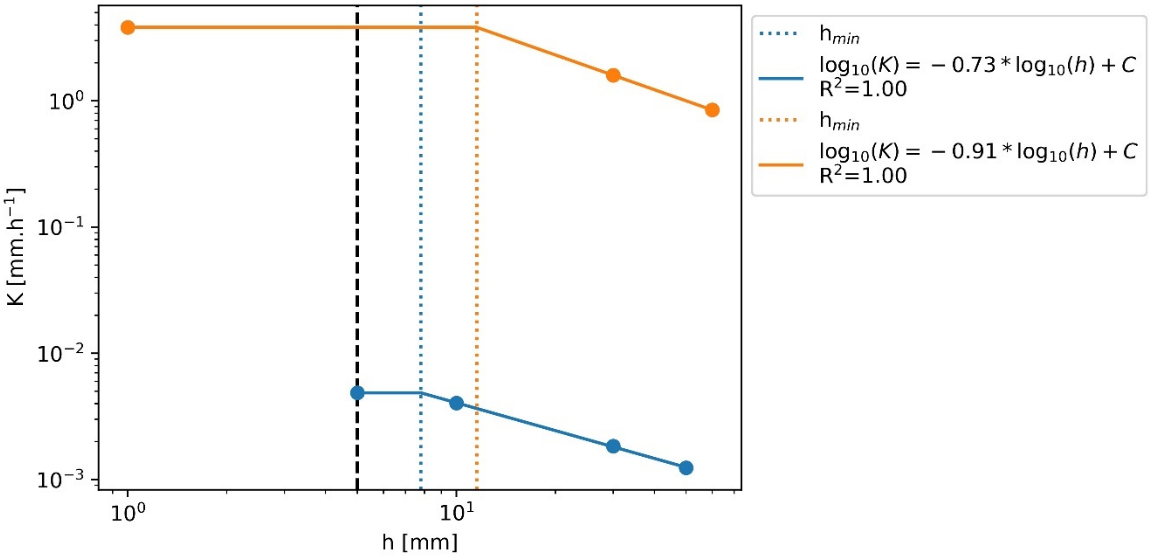

Figure 1: Two e~~E~~xamples ~~of~~ for the linear fit in log-log space. The colors denote two different measured tension series. The filled circles correspond to measured K_h, while the lines indicate the interpolation carried out by the model. The bold black dashed line marks a supply tension of 5 mm. K_h at tensions between 0 and 5 mm were assumed to be identical

to K_s. Reported K_s values were assigned a tension of 1 mm for illustration purposes. The equations for the linear part of the fit are shown in the legend. C represents the intercept with the y-axis of the linear fit in log-space, h_{min} corresponds to the supply tension at which the largest pores in the soil are water-filled.

Following Jarvis et al., 2013, we interpolated K_h for tensions in-between the ones measured in the source publications. We achieved this by fitting a log-log linear model with a kink at a tension h_{min}, which denotes the tension at which the largest effective pores in the soil are water-filled (see Figure 1). Therefore, K_h ≡~~==~~ K_s for all tensions $h \le h_{min}$. If K_s was not measured but instead a K_h value at $h \le 5$ mm was available, K_s was set to the available K_h value (Figure 1 orange line). In cases where more than one K_h value was measured at a tension smaller or equal to 5 mm (including h = 0 mm, i.e. K_s), we averaged them and fixed K_s and K_h for $h \le h_{min}$ to the average (Figure 1 green line). K_h values at h > 5 mm were used to fit the log-log linear relationship. The tension at which the fitted log-log slope intersected with K_s defined h_{min}. We used the fitted model to estimate all K_h values for tensions for $10 \le h \le 100$ mm at 10 mm intervals. The K_h values were only interpolated between the tensions that were measured in the source publication. The only exceptions from this rule were made in the case where a K_h value for a tension of 80 or 90 mm was provided together with at least one other K_h value measured at a smaller tension. Then, the missing K_h values were extrapolated up to a tension of 100 mm. Figure 1 shows examples of model fits. Only entries with an R^2 greater or equal to 0.9 were retained in the analysis.

2.2 Data availability and spatial coverage

Although 92% of the OTIM data ~~is~~ are from ~~the~~ topsoils, ~~it~~ OTIM also contains some data points measured at greater soil depths. In the following meta-analysis, only measurements from the topsoil were included to prevent bias and all datasets measured at soil depths below 200 mm were removed. Last but not least, we found that the relationship between supply tension and K_h was distorted if data entries were included that did not cover the complete tension range from h = 0 to 100 mm. Possible reasons for the difficulties to match K_h data from tension series with different lengths are discussed at the beginning of the results and discussion section. Otherwise, we focused on data entries that included K_h values for the complete tension range in the exploratory data analysis and the meta-analyses. The available datasets after these filtering steps correspond to the ones indicated in blue (and termed 'focus') in the following figures.

Most tension-disk infiltrometer studies were conducted in Europe, North America and Southeast Australia (Figure 2). Clearly, fewer studies have been carried out in Asia, South America and Africa. The lack of datasets from Russia, Mesoamerica, the arctic regions and the tropics is remarkable. This geographical bias is aggravated if only measurements on the topsoil are considered that allow inferences about K_h for the complete range of tensions ($0 \leq h \leq 100$ mm) with a sufficiently good coefficient of determination. Then, all the data entries collected in southern South America and south-eastern Australia were omitted, as well. Overall, the data in OTIM mostly stem from temperate climate regions.

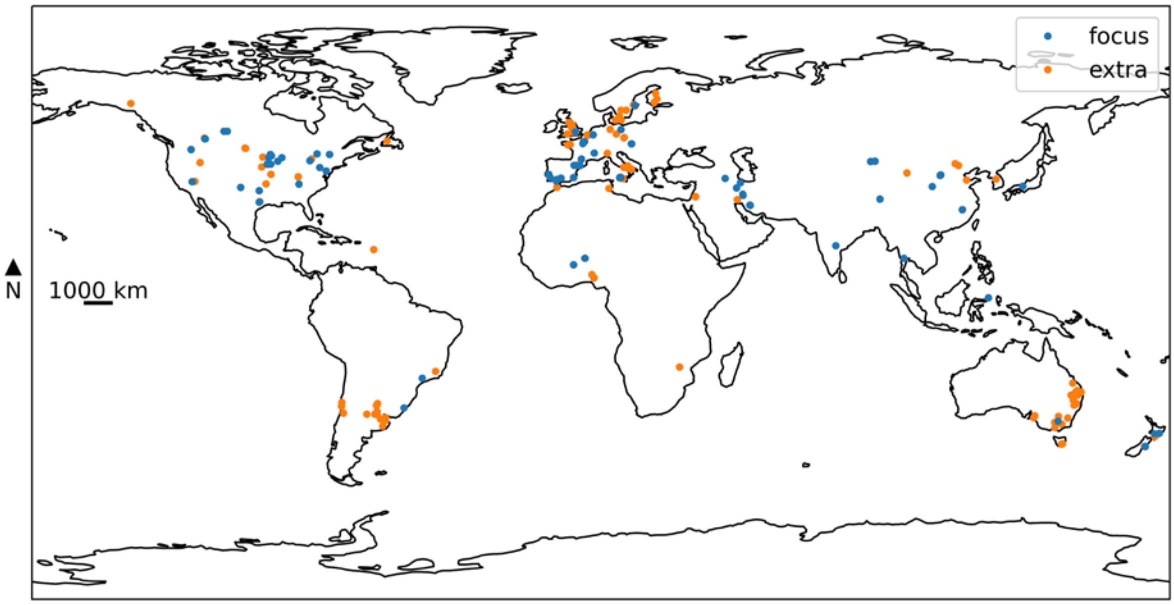

Figure 2: Map of the study locations collected in the OTIM. The values are shown for the filtered entries ('focus') and in parenthesis for all the entries available in the database ('focus' and 'extra').

Figure 3 depicts the number of K_h values available for $0 \leq h \leq 100$ mm. These figures represent the hydraulic conductivities derived from the log-log linear model presented above, not the raw data measured and reported in the source publications. A large number of entries span the full range of tensions of interest (0 to 100 mm), whereas a smaller number of entries only have data up to a tension of 60 mm. Often, but not always, such data series were obtained with the widely available Mini-Disk infiltrometer distributed by the *Meter* group (formerly by *Decagon*), which is limited to tensions h ≤ 70 mm. An overview on the metadata included in OTIM is given in Table 2. Data gaps are present, especially for bulk density and for information on the soil management at the study site, apart from tillage operations. Note that the annual mean temperature and precipitation are only two examples representing the climatic variables enumerated in section 2.3. There are very few missing values for the climate data, since it was estimated from the coordinates of the study sites. The same holds for the elevation data and information on the WRB soil type.

Table 2: Number of entries and gaps for each feature along with units and range (if continuous) or choices (if categorical). The values are shown for the filtered entries (‘focus’) and in parenthesis for all the entries available in the database (‘focus’ and ‘extra’).

Type	Predictor	Unit	Range/Choices	Number of entries	Number of gaps
Soil	Sand content	kg kg^{-1}	0.0 -> 0.9 (0.0 -> 1.0)	402 (1070)	64 (215)
Soil	Silt content	kg kg^{-1}	0.0 -> 0.8 (0.0 -> 0.8)	402 (1070)	64 (215)
Soil	Clay content	kg kg^{-1}	0.0 -> 0.7 (0.0 -> 0.8)	405 (1107)	61 (178)
Soil	Bulk density	g cm-3	0.5 -> 1.8 (0.1 -> 2.2)	324 (771)	142 (514)
Soil	Soil organic carbon	kg kg^{-1}	0.0 -> 0.1 (0.0 -> 1.0)	339 (938)	127 (347)
Climate	Annual mean temperature	°C	-0.4 -> 29.1 (-3.8 -> 29.1)	466 (1214)	0 (71)
Climate	Annual mean precipitation	mm	22.0 -> 3183.0 (22.0 -> 3183.0)	466 (1214)	0 (71)
Climate	Average aridity index	-	0.0 -> 1.9 (0.0 -> 2.8)	466 (1214)	0 (71)
Climate	Precipitation seasonality (CV)	-	9.9 -> 138.5 (9.6 -> 138.5)	466 (1214)	0 (71)
Climate	Mean diurnal range	ºC	6.9 -> 18.2 (4.8 -> 18.5)	466 (1214)	0 (71)

Management	Land use	-	arable, bare, grassland, woodland/plantation	453 (1249)	13 (36)
Management	Tillage	-	conventional tillage, no tillage, reduced tillage	422 (1190)	44 (95)
Management	Soil compaction	-	compacted, not compacted	76 (265)	390 (1020)
Management	Sampling time	-	soon after tillage, consolidated soil	367 (993)	99 (292)

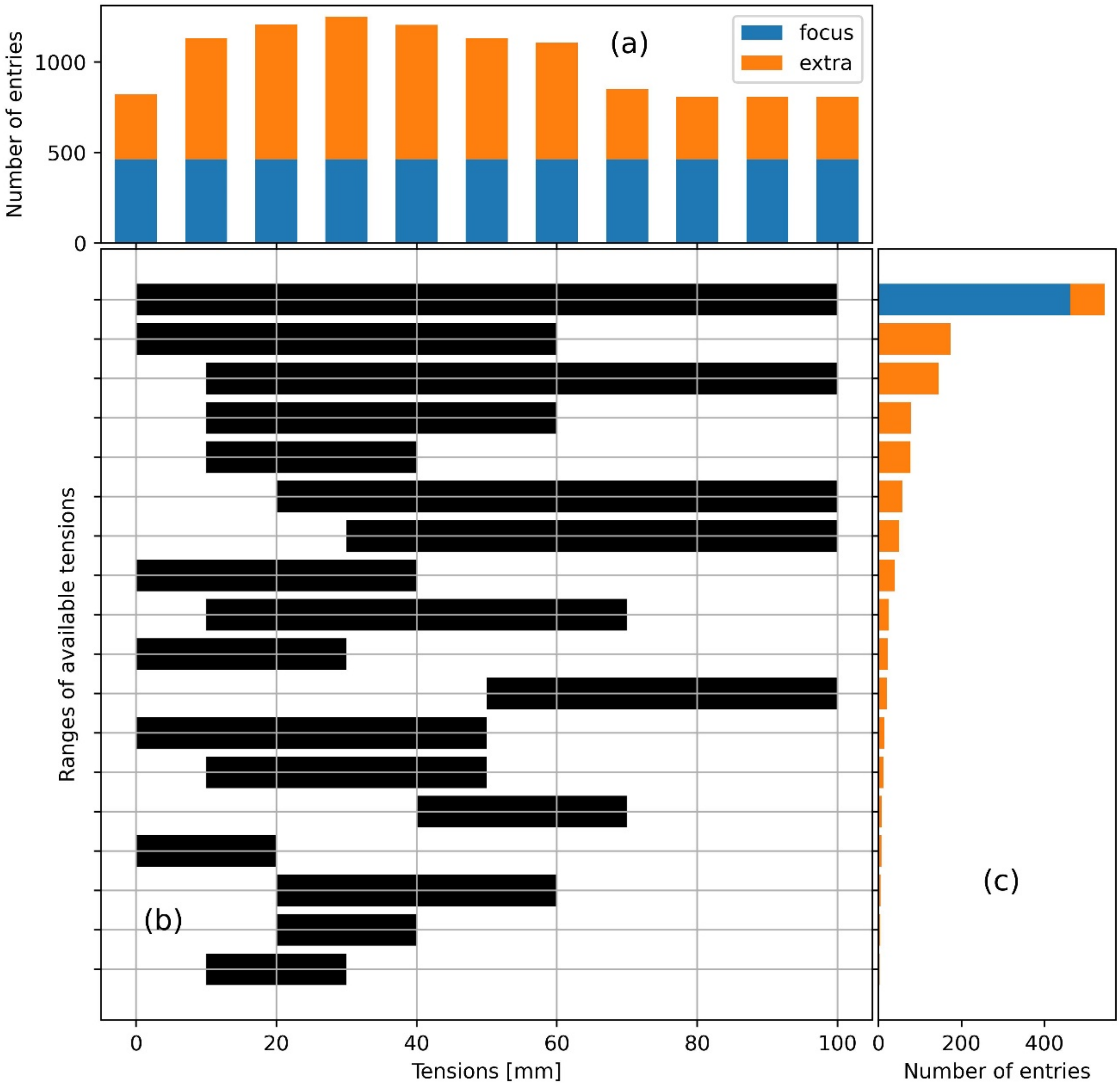
(a)
focus
extra
Number of entries
0
500
1000
(b)
Ranges of available tensions
0
20
40
60
80
100
Tensions [mm]
(c)
0
200
400
Number of entries

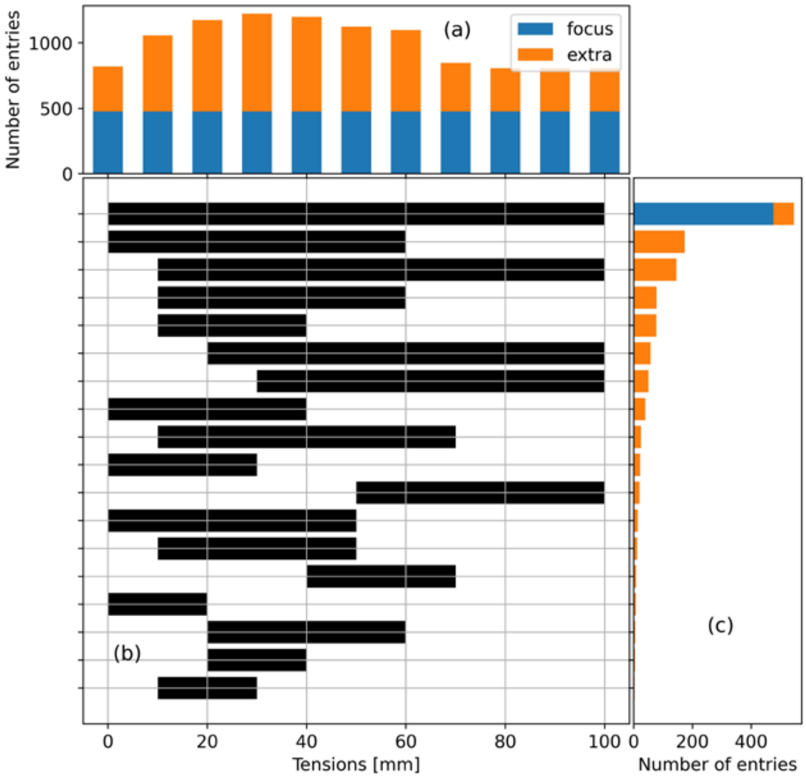

Figure 3: (a) number of available K_h values per supply tension, (b) ~~range~~ available tension series with the black bar indicating the span between T_{min} and T_{max}~~of available tensions and~~ (c) their respective ~~occurrence~~ frequency in the database. The values are shown for the filtered entries ('focus') and ~~in parenthesis~~ for all the entries available in the database ('focus' and 'extra').

The metadata for the datasets used in the exploratory data analysis are summarized in Figure 4. OTIM contains predominantly data from arable fields. The distributions of the climate variables confirms that the data in OTIM was also mostly acquired in temperate climates, with a bias towards the somewhat drier climates that are most typical for arable land. The soil texture, bulk density and organic carbon content data also appear reasonably representative for soils in this climate zone.

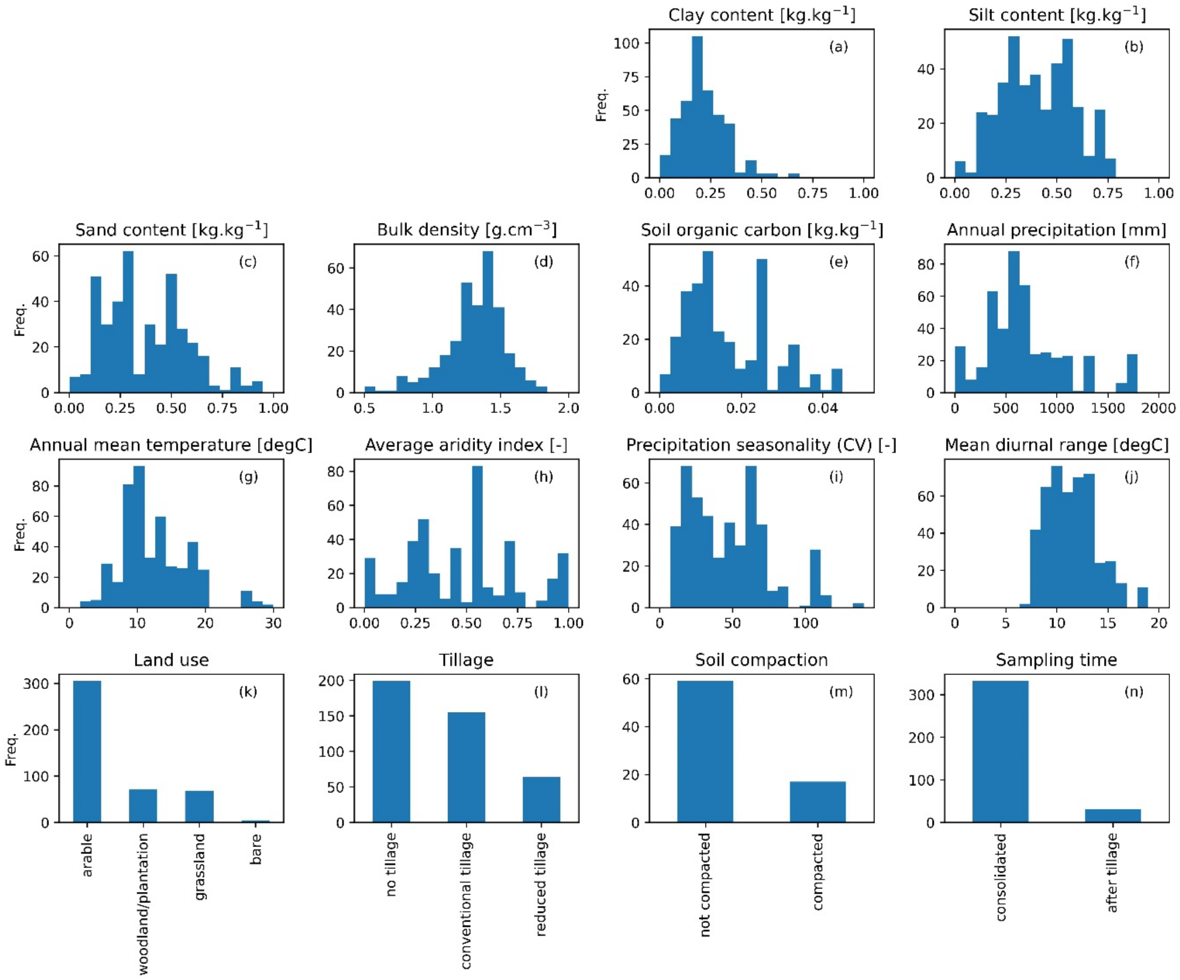
Clay content [kg.kg^{-1}]
(a)
Silt content [kg.kg^{-1}]
(b)
Sand content [kg.kg^{-1}]
(c)
Bulk density [g.cm^{-3}]
(d)
Soil organic carbon [kg.kg^{-1}]
(e)
Annual precipitation [mm]
(f)
Annual mean temperature [degC]
(g)
Average aridity index [-]
(h)
Precipitation seasonality (CV) [-]
(i)
Mean diurnal range [degC]
(j)
Land use
(k)
arable
woodland/plantation
grassland
bare
Tillage
(l)
no tillage
conventional tillage
reduced tillage
Soil compaction
(m)
not compacted
compacted
Sampling time
(n)
consolidated
after tillage
Freq.

274

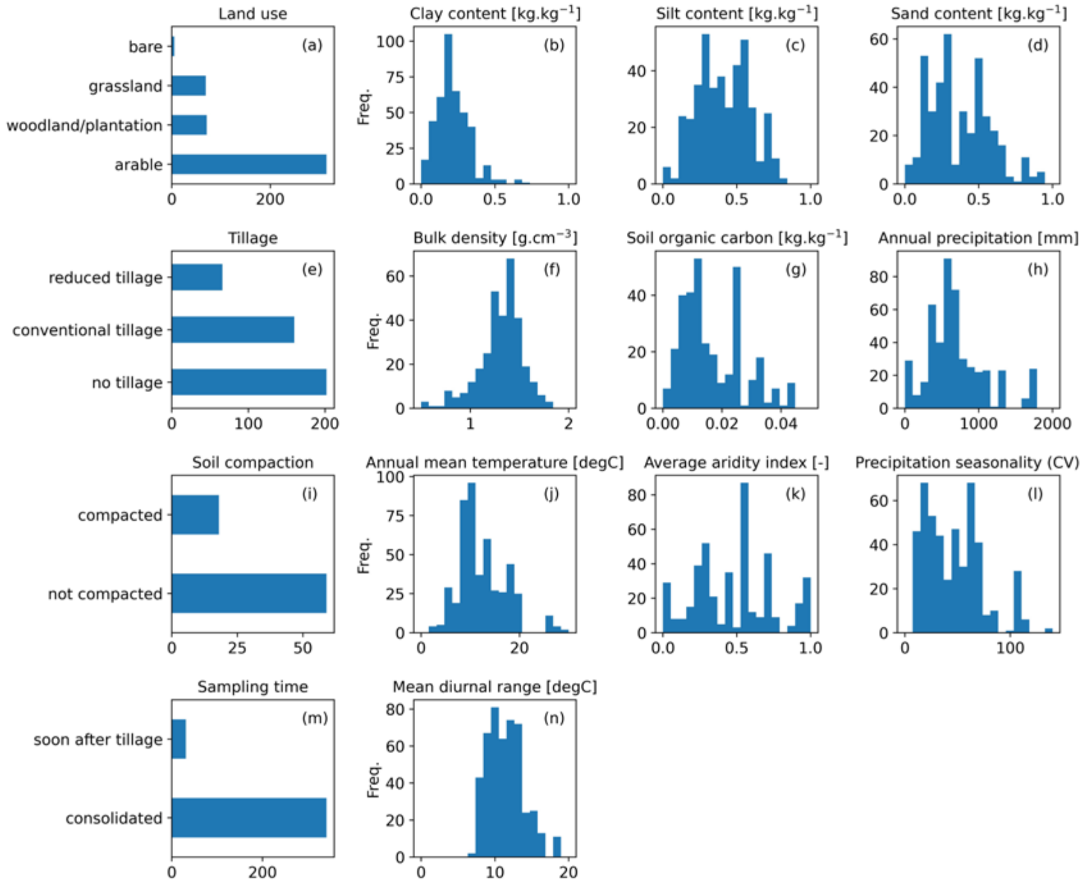

Figure 4: Distributions of continuous and categorical variables in the 'focus' dataset.

2.3 Exploratory data analysis

Some source publications only provided a few data entries for K_h, sometimes only comparing two different treatments, while other source studies contain data for a larger number of treatments and/or sites. In some publications, data for all individual tension-disk measurements are available, even if replicates were measured. In others, only averages of the replicated measurements are reported, while still others yield average K_h values for individual replicated treatment blocks. This makes appropriate data weighting complicated, but also extremely important when analysing the meta-dataset. It also introduces uncertainty, because it is not always clear whether the replicated averages were calculated using the geometric or the arithmetic mean. Considering that hydraulic conductivities at or near saturation are known to be log-normally distributed, the former would be best. In the following, we assumed that geometric averaging was used when replicated values were reported in source publications. In the following, we calculated data weights as

$$\omega_i = \frac{n_{r,i}}{\sqrt{N_i}} \qquad \text{Equation 1}$$

where ω_i is the weight for data entry *i*, $n_{r,i}$ is the number of replicates from which the values of *i* were averaged and N_i is the total number of measurements included in the publication from which data entry *i* was obtained. With this approach, we up-weighted data entries according to the number of replicate measurements from which they were averaged and down-weighted the impact of studies that published larger amounts of data.

We used weighted Spearman rank correlation coefficients to investigate relationships between continuous variables. We considered correlations significant if they exhibited p-values of less than 0.05. The latter were determined numerically by running randomization tests with 200 repetitions.

2.4 Meta-analysis

Data entries in OTIM with specific land use or management were very unevenly distributed. For example, the large majority of data was measured on sites with land use ‘arable’ (see Figure 4a). Such uneven distributions may lead to bias when averaged over all entries of a specific feature in exploratory data analyses. We therefore investigated the effects of land use and management as well as soil compaction and time of measurement on K_h with the aid of pairwise comparisons published within individual studies and calculated effect sizes (*ES*) for each investigated class.

To reduce bias arising from the varying number of data entries published within individual studies, we grouped all entries according to the factors land use, tillage, compaction, and sampling time. Here we only considered binary pairs, that is arable or not arable in the case of land use and tilled or not tilled, compacted or not compacted as well as ‘measured soon after tillage’ or ‘measured on consolidated soil’ for the other three factors. In addition, we checked whether different entries within individual studies stemmed from the same or a very similar site. We did this by comparing the respective USDA texture classes and a climate variable, namely the aridity class. All data entries within each individual study that exhibited identical land use, soil management, soil compaction, sampling time, texture and aridity were averaged and the number of corresponding replicates was summed.

For each binarized factor (e.g. tillage), a *control* value was chosen (e.g. zero tillage). All values different from the control represent the *treatment* (e.g. conventional tillage and reduced tillage). Within individual studies, pairs among the averaged entries were formed for each combination of a control and a treatment value. These pairs were used to compute the effect size. Following Basche ~~&~~and DeLonge (2019), we defined the effect sizes as the log10 of the ratio of $K_{h,t}$ of the treatment divided by $K_{h,c}$ of the control

$$ES_l = log_{10}\left(\frac{K_{h,t}}{K_{h,c}}\right) \qquad \text{Equation 2}$$

where the subscript l indicates the l^{th} pair for which the effect size was computed and the indices '*t*' and '*c*' stand for treatment and control, respectively. The average effect size *ES* for each of the four investigated factors was calculated as the weighted mean of the individual ES_l using the weight

$$w_l = \frac{\nu_c\,\nu_t}{\nu_c + \nu_t} \qquad \text{Equation 3}$$

where the subscript l indicates again the l^{th} pair for which the effect size was computed and ν_c and ν_t denote the number of (summed) replicates for control and treatment, respectively. In addition, we calculated the weighted standard error

$$\sigma_{\bar{ES}} = \sqrt{\frac{\sum_{i=0}^{n} \; w_l\left(ES_l - \overline{ES}\right)^2}{\frac{n-1}{n}\sum_{l=0}^{n} \; w_l}} \qquad \text{Equation 4}$$

where $\overline{ES}$ is the mean effect size. Table 3 summarises the evaluated factors, the number of pairs involved and the number of different studies from which the pairs were obtained.

To estimate the robustness of the effect size, we carried out a sensitivity analysis using the Jackknife technique, similarly to Basche ~~&~~and DeLonge, 2019. This method aims to show the sensitivity of the averaged effect size to data from specific studies. For each factor, a given number of studies was randomly picked and removed from the dataset. The averaged effect size and its standard error ~~was~~ were computed with the rest of the dataset. The process started by removing one study, after which up to nine more studies were removed. This random selection was repeated 50 times to rule out bias. The average of the means and standard errors for the 50 realisations was computed and plotted. Observed effect sizes were judged trustworthy if they did not change after removal of studies to calculate them. We constrained the sensitivity analyses in our study to the effect sizes for K_s and K_{100}.

Table 3: Number of studies and paired comparison with their respective control and treatment values used for the meta-analysis exemplary for the K_{100} values.

Factor	**Control**	**Treatments**	**Studies**	**Paired comparisons**
Land use	not arable	arable	10	24
Tillage	no tillage	conventional tillage, reduced tillage	15	32
Compaction	not compacted	compacted	6	8
Sampling Time	consolidated soil	soon after tillage	6	12

3 Results and discussion

3.1 Differences between data entries with different tension ranges

If all data are considered (‘focus’ and ‘extra’), Figure 3 illustrates that approximately 40% of the data in OTIM provided K_h for every h with $0 \leq h \leq 100$ mm. For another 40%, K_h was only measured in the wet range, i.e. at tensions below 70 mm. The remaining K_h data was only acquired at the dry range. Here, we counted all data entries for which K_s were not measured and could not be estimated. Figure 5 shows how data from entries with complete, dry and wet ranges differed. The K_h for the wet range receded faster with increasing tension than series that also included measurement in the dry range. A large portion of these datasets were obtained with the Mini-Disk infiltrometer. However, a closer inspection of the impact of the disk diameters used to acquire the respective K_h did not confirm suspicions that the bias was related to the use of this special type of infiltrometer (see Figure 6a). The observed differences between the K_h curves could have been introduced by co-correlations with soil texture or climate. Another explanation may be experimenter bias, since individual research groups tend to use specific tension ranges for more than one study. In this study, however, we focused solely on data entries for which we were able to reconstruct K_h for all h in between 0 and 100 mm supply tension in the following exploratory data analyses and meta-analyses. This greatly facilitated the data interpretation.

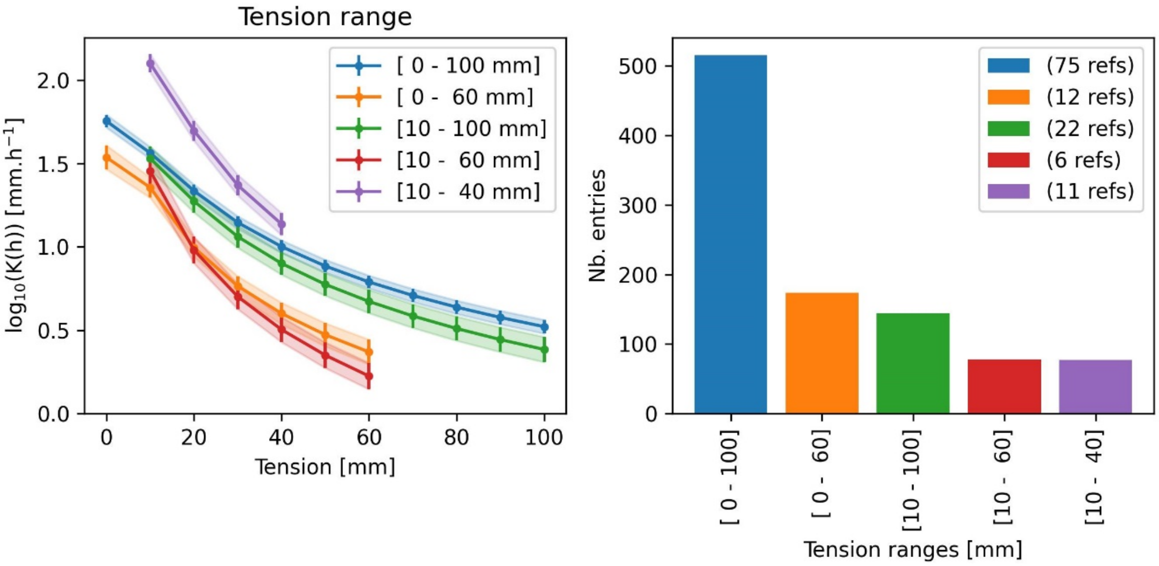

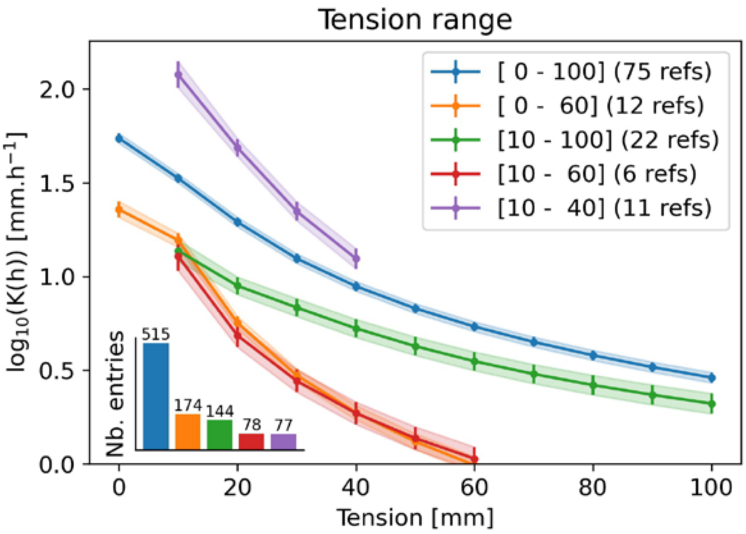

Figure 5: Evolution of weighted mean *K_h* with tension available in OTIM, sorted by the tension range the data was spanning. The number of publications from which the data originated is shown between parentheses in the legend. The shaded areas and the error bars represent the weighted standard error of the mean.

3.2 Statistical relationships between K_h and methods used

Figure 6a confirms that the diameter of the tension disk did not have a systematic impact on the results. The majority of the data were collected starting under dry conditions (large tensions) and subsequently measured under increasingly wet conditions (smaller tensions). Figure 6b illustrates that beginning the experiment under wet conditions is associated with larger hydraulic conductivities at identical supply tensions. This is well known and is referred to as hysteresis, which is due to ink-bottle effects, impacts of water repellency, air entrapment and swelling of clay particles (Hillel, 2004). Figure 6c shows that the large majority of studies used the ‘steady-state piecewise’ method to solve the Wooding equation and convert the measured infiltration rates to hydraulic conductivities. This method leads to smaller K_h for larger tensions than the other methods. The ‘transient’ and ‘steady-state constant’ methods yielded larger K_h in the unsaturated range. For the latter method, it is known that it overestimates unsaturated K_h (Jarvis et al., 2013). We tested whether excluding data from ‘transient’ and ‘steady-state constant’ methods changed the results of the meta-analyses, but found that they only changed to a minor degree. Data from all methods were therefore included in the following. Note that the ‘transient’ method was mostly applied in conjunction with Mini-Disk Infiltrometers, albeit the respective data is not included in Figure 6 since it does not span the entire suction range.

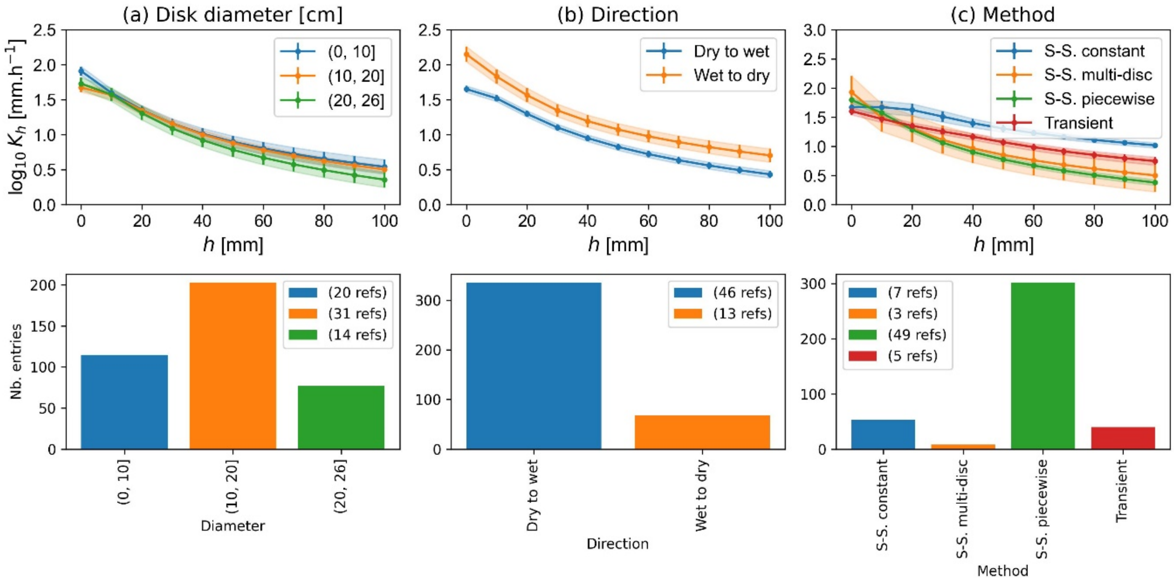

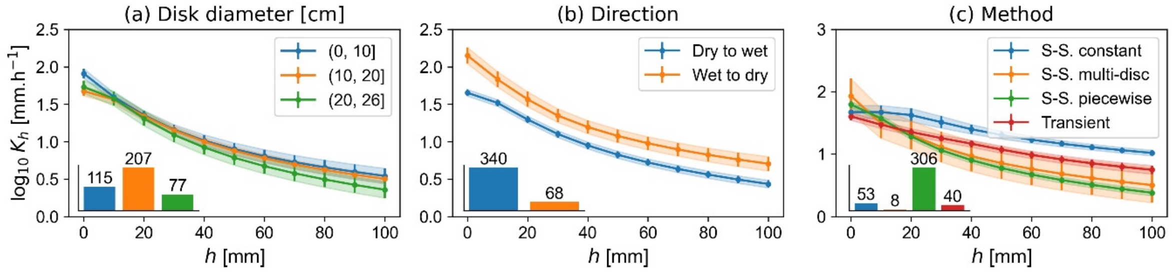

Figure 6: Evolution of weighted mean K_h as a function of applied tension for (a) disk diameter, (b) direction and (c) method of fitting. ‘S.-S.’ stands for ‘steady-state’. More specifically, the method ‘S.-S. constant’ is outlined in Logsdon and Jaynes (1993), ‘S.-S. multi-disc’ in Smettem and Clothier (1989), and ‘S.-S. piece-wise’ in Reynolds and Elrick (1991) or Ankeny et al. (1991) and ‘Transient’ in Zhang (1997) or Vandervaere et al. (2000).

The shaded areas and the error bars represent the weighted standard error of the mean.The bar plots in each subplot indicate how many data points of each class were in the data set.

3.3 Correlation between K_h at different tensions

The fact that correlations between K_h estimated at supply tensions between 40 and 100 mm were relatively stable (Table 4) indicates that the respective flow paths and/or mechanisms remained very similar in this tension range. However, these correlations weakened at tensions between 10 and 20 mm, giving rise to the existence of a threshold above which water flow in the largest macropores becomes the dominant flow mechanism. The poor correlation between K_s and K_h at larger supply tensions is in line with findings that K_s is not well suited to infer to soil unsaturated hydraulic conductivities (Schaap and Leij, 2000).

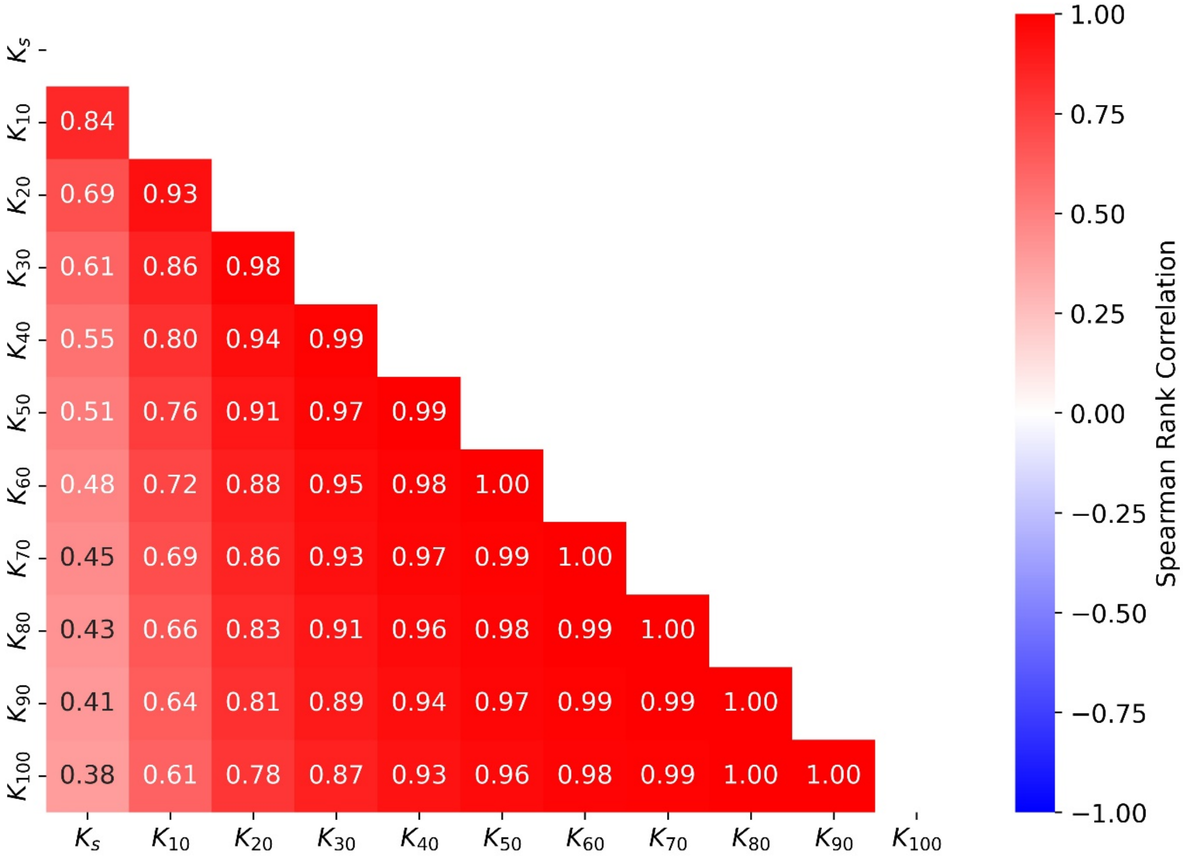

	K_s	K_{10}	K_{20}	K_{30}	K_{40}	K_{50}	K_{60}	K_{70}	K_{80}	K_{90}	K_{100}
K_s											
K_{10}	0.84										
K_{20}	0.69	0.93									
K_{30}	0.61	0.86	0.98								
K_{40}	0.55	0.80	0.94	0.99							
K_{50}	0.51	0.76	0.91	0.97	0.99						
K_{60}	0.48	0.72	0.88	0.95	0.98	1.00					
K_{70}	0.45	0.69	0.86	0.93	0.97	0.99	1.00				
K_{80}	0.43	0.66	0.83	0.91	0.96	0.98	0.99	1.00			
K_{90}	0.41	0.64	0.81	0.89	0.94	0.97	0.99	0.99	1.00		
K_{100}	0.38	0.61	0.78	0.87	0.93	0.96	0.98	0.99	1.00	1.00	

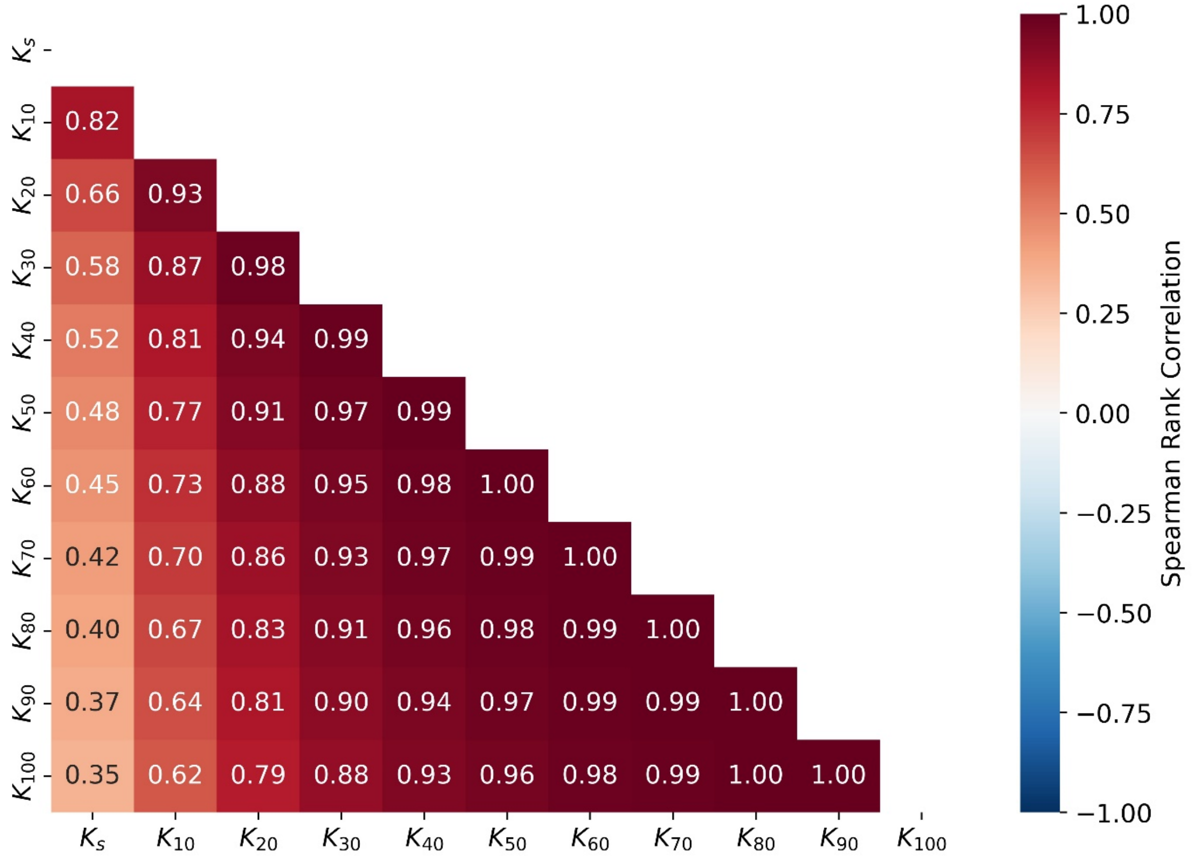

	K_s	K_{10}	K_{20}	K_{30}	K_{40}	K_{50}	K_{60}	K_{70}	K_{80}	K_{90}	K_{100}
K_s											
K_{10}	0.82										
K_{20}	0.66	0.93									
K_{30}	0.58	0.87	0.98								
K_{40}	0.52	0.81	0.94	0.99							
K_{50}	0.48	0.77	0.91	0.97	0.99						
K_{60}	0.45	0.73	0.88	0.95	0.98	1.00					
K_{70}	0.42	0.70	0.86	0.93	0.97	0.99	1.00				
K_{80}	0.40	0.67	0.83	0.91	0.96	0.98	0.99	1.00			
K_{90}	0.37	0.64	0.81	0.90	0.94	0.97	0.99	0.99	1.00		
K_{100}	0.35	0.62	0.79	0.88	0.93	0.96	0.98	0.99	1.00	1.00	

Table 4: Weighted Spearman rank correlation coefficients between K_h at different tensions. Correlation coefficients are shown up to p-values of 0.001.

3.4 Statistical relationships between K_h and soil properties

Soils with coarse texture exhibited larger K_h in the unsaturated range, which is caused by the large and abundant primary pores in between individual sand grains (Figure 7a). At saturation, the average hydraulic conductivity of all three texture classes was similar. This is explained by the presence of large structural pores in the medium and fine-textured soils. Medium-textured soils had the lowest K_h in the investigated range of tensions, which may be due to a denser soil matrix in loamy soils and a lower structural stability of silty soils. Larger bulk densities decreased K_h across the whole range of investigated tensions, which reflects the reduced porosity with increasing bulk density (Figure 7b).

The hydraulic conductivity in the saturated and near-saturated range is especially affected by soil compaction, which predominantly reduces the abundance and connectivity of macropores (Pagliai et al., 2004; Whalley et al., 1995). Large bulk densities are also known to reduce burrowing activities of the soil macrofauna (Capowiez et al., 2021) as well as root growth (Lipiec ~~&~~and Hatano, 2003), also leading to less abundant and less connected large macropores. An increase in the soil organic carbon content was connected with smaller K_h at the dry end of the investigated tension range if soils with organic carbon contents of more than 0.03 kg.kg^{-1} were excluded (Figure 7c). This decrease may be explained by water repellency, which is generally positively correlated with organic carbon content. A similar observation was already reported in Jarvis et al.~~,~~ (2013). Note that no major correlations of SOC with soil texture were observed in the investigated dataset (Table 5). For soils with organic carbon contents larger than 0.03 kg.kg^{-1}, K_h increased once again. This may indicate that, above this threshold, better-developed macropore networks associated with large SOC contents (e.g. Larsbo et al., 2016b) outweighed any effects of water repellency.

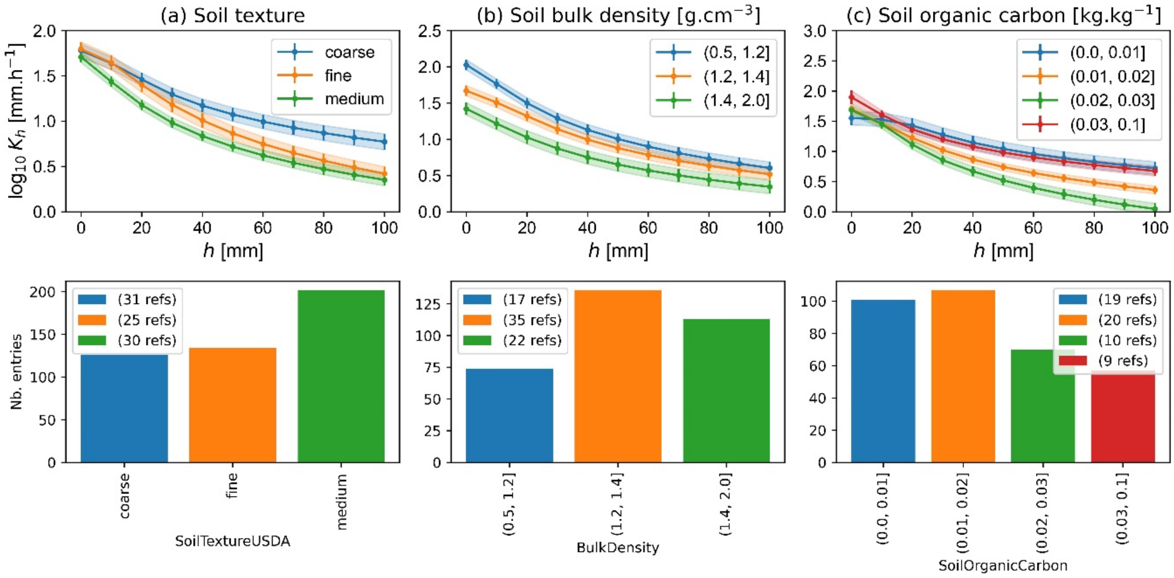

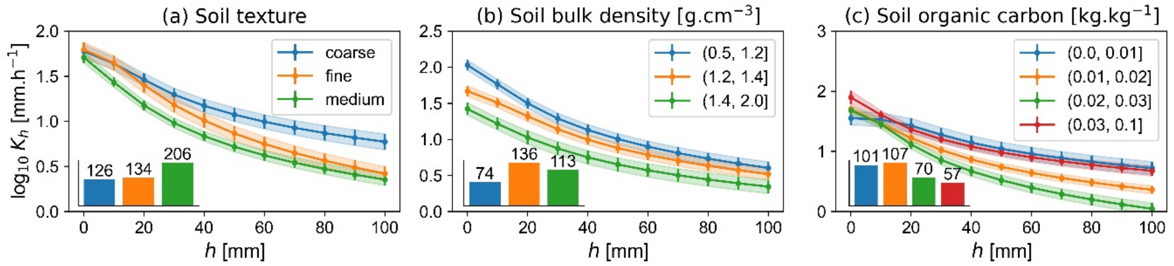

Figure 7: Evolution of weighted mean K_h as a function of applied tension for (a) soil texture, (b) soil bulk density and (c) soil organic carbon. The shaded areas and the error bars represent the weighted standard error of the mean. The soil textures were classified using USDA texture classes as follows: fine (clay, clay loam, silty clay, silty clay loam), medium (silt loam, loam), coarse (loamy sand, sand, sandy clay, sandy clay loam, sandy loam). The bar plots in each subplot indicate how many data points of each class were in the data set.

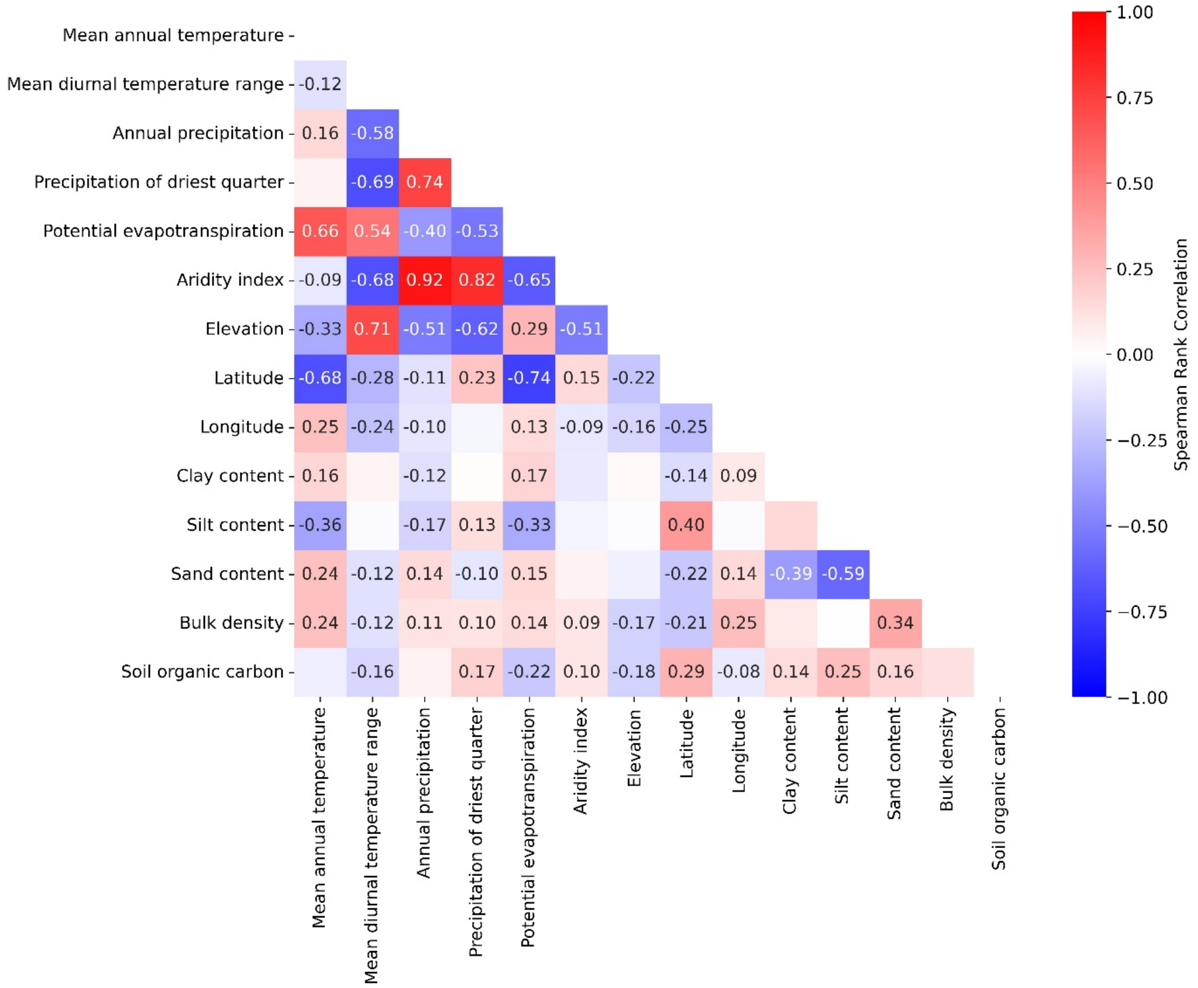

	Mean annual temperature	Mean diurnal temperature range	Annual precipitation	Precipitation of driest quarter	Potential evapotranspiration	Aridity index	Elevation	Latitude	Longitude	Clay content	Silt content	Sand content	Bulk density	Soil organic carbon
Mean annual temperature														
Mean diurnal temperature range	-0.12													
Annual precipitation	0.16	-0.58												
Precipitation of driest quarter		-0.69	0.74											
Potential evapotranspiration	0.66	0.54	-0.40	-0.53										
Aridity index	-0.09	-0.68	0.92	0.82	-0.65									
Elevation	-0.33	0.71	-0.51	-0.62	0.29	-0.51								
Latitude	-0.68	-0.28	-0.11	0.23	-0.74	0.15	-0.22							
Longitude	0.25	-0.24	-0.10		0.13	-0.09	-0.16	-0.25						
Clay content	0.16		-0.12		0.17			-0.14	0.09					
Silt content	-0.36		-0.17	0.13	-0.33			0.40						
Sand content	0.24	-0.12	0.14	-0.10	0.15			-0.22	0.14	-0.39	-0.59			
Bulk density	0.24	-0.12	0.11	0.10	0.14	0.09	-0.17	-0.21	0.25			0.34		
Soil organic carbon		-0.16		0.17	-0.22	0.10	-0.18	0.29	-0.08	0.14	0.25	0.16		

Table 5: Weighted Spearman rank correlation coefficients between climate variables, elevation above sea level and soil properties. Correlation coefficients are shown up to p-values of 0.001.

3.5 Statistical relationships between K_h and climate variables

One important observation made in recent years was that saturated and near-saturated hydraulic conductivities correlated strongly with climate variables (Jarvis et al., 2013; Jorda et al., 2015; Hirmas et al., 2018). Table 6 gives an overview of weighted Spearman rank correlations between K_h and six of the 20 climate variables included in OTIM that exhibited the strongest correlations with K_h. The elevation of the sampling site above sea level, its latitude and longitude, soil texture, bulk density and soil organic carbon content are also shown for comparison. It is striking that the soil properties were less well correlated with K_h than some of the climate variables. Of the three USDA texture fractions, the clay content was negatively and the sand content positively correlated with K_h at the drier investigated tension range, while no significant correlations were found for the silt fraction (Table 6). Only the bulk density exhibited correlation coefficients as large as the climate variables.

The largest absolute values of the weighted rank correlations were observed for the mean diurnal range of temperature and the aridity index. Both reach a maximum at the dry end of the considered tension range, i.e. for K_{100}, with correlation coefficients of 0.43 and -0.4, respectively. Table 5 reveals that both of these best correlated climate variables were accidently correlated with choices in experimental design and data evaluation made by the investigators in the respective source studies that will amplify these observed correlations to K_h. However, if a smaller dataset is considered in which such methodological bias as well as potential bias due to differences in land use were eliminated, the correlations persisted (Table B1). We therefore infer that the observed effect of climate on K_h is real.

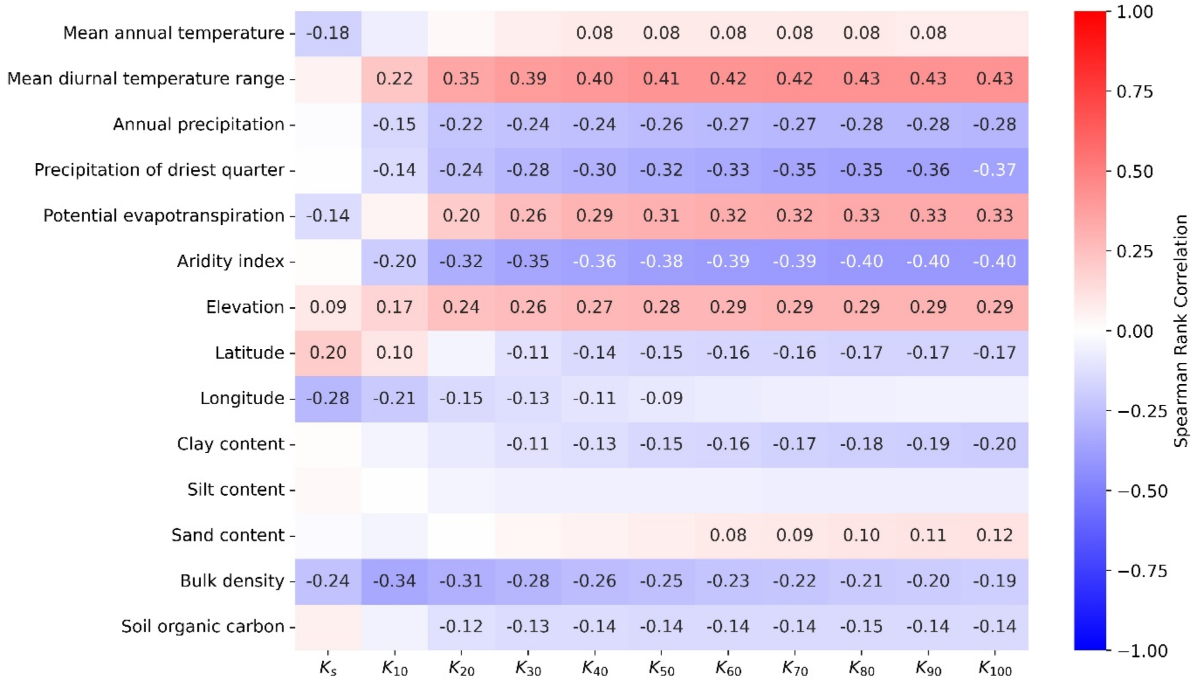

	K_s	K_{10}	K_{20}	K_{30}	K_{40}	K_{50}	K_{60}	K_{70}	K_{80}	K_{90}	K_{100}
Mean annual temperature	-0.18				0.08	0.08	0.08	0.08	0.08	0.08	
Mean diurnal temperature range		0.22	0.35	0.39	0.40	0.41	0.42	0.42	0.43	0.43	0.43
Annual precipitation		-0.15	-0.22	-0.24	-0.24	-0.26	-0.27	-0.27	-0.28	-0.28	-0.28
Precipitation of driest quarter		-0.14	-0.24	-0.28	-0.30	-0.32	-0.33	-0.35	-0.35	-0.36	-0.37
Potential evapotranspiration	-0.14		0.20	0.26	0.29	0.31	0.32	0.32	0.33	0.33	0.33
Aridity index		-0.20	-0.32	-0.35	-0.36	-0.38	-0.39	-0.39	-0.40	-0.40	-0.40
Elevation	0.09	0.17	0.24	0.26	0.27	0.28	0.29	0.29	0.29	0.29	0.29
Latitude	0.20	0.10		-0.11	-0.14	-0.15	-0.16	-0.16	-0.17	-0.17	-0.17
Longitude	-0.28	-0.21	-0.15	-0.13	-0.11	-0.09					
Clay content				-0.11	-0.13	-0.15	-0.16	-0.17	-0.18	-0.19	-0.20
Silt content											
Sand content							0.08	0.09	0.10	0.11	0.12
Bulk density	-0.24	-0.34	-0.31	-0.28	-0.26	-0.25	-0.23	-0.22	-0.21	-0.20	-0.19
Soil organic carbon			-0.12	-0.13	-0.14	-0.14	-0.14	-0.14	-0.15	-0.14	-0.14

Table 6: Weighted Spearman rank correlation coefficients between K_h at different tensions and climatic features and soil properties. Correlation coefficients are shown up to p-values of 0.001.

The annual mean diurnal temperature range and the aridity index were strongly correlated with each other, with a weighted correlation coefficient of -0.68 (Table 5). Strong correlations to at least one of these two variables with absolute values >0.6 were also found for most of the investigated climate variables. It is therefore difficult to separate the climate effects due to these strong inter-correlations. Nevertheless, it is striking that the mean annual diurnal temperature ranges are much better correlated with K_{100} than the mean annual temperature itself (Table 6). In addition, the mean annual precipitation in the driest quarter of the year and the precipitation in the driest quarter of the year exhibited stronger correlations than the mean annual precipitation. It appears that temperature and precipitation fluctuations are more strongly coupled to near-saturated hydraulic conductivities than the absolute temperatures or precipitation amounts.

Among possible reasons for the observed correlations may be increased splash erosion during heavy rainfalls that are common in regions with large precipitation seasonality, more soil compaction in wetter climates due to trafficking, a larger vertical burrowing activity of soil fauna in climates with large diurnal temperature ranges, more vertically oriented root systems in arid climates or climate specific choices in land use and soil management. The data in OTIM cannot provide an answer to these questions. Investigations of such relationships should be the focus of future studies.

Another site factor that is positively correlated with K_h is the elevation above sea level (Table 6). Notably, elevation above sea level also was found to be an important predictor for K_s in Gupta et al. (2021b), which suggests that there are indeed pedogenetic reasons behind the observed correlation. In the case of infiltrometer measurements, the decreased atmospheric pressure with height on the supply tension can be neglected. The supply tension is always equivalent to the weight of the water column adjusted in the bubbling tower. The weight of the water column will be smaller due to the general decrease of earth's gravitational constant with height due to a larger centrifugal force. However, the weight of the water column would only be reduced by approximately one or two percent. Also, indirect influences of larger heights on the infiltration rate cannot explain the observed correlation. A lower temperature would make the water column denser. However, the effect would be less than 1% in the relevant temperature range. In contrast, a lower temperature would increase the viscosity of water to a much larger degree, e.g. by up to approximately 30% between temperatures of 10 and 20 ^{o}C. The temperature effect should thus lead to a negative correlation between elevation and K_h, which is the opposite of what was observed. Bias in the K_h measurements due to such physical effects can thus be ruled out. Elevation may instead be a proxy for well-drained soils, as stagnant soil water and high groundwater tables are less likely with height above sea level. This may favour soil life and better developed root systems and decrease risks of compaction when the soil is trafficked.

The observed correlations of K_h with latitude and longitude probably reflect co-correlations with climate variables together with experimenter bias, since it appears likely that approaches in setting up tension disk infiltrometers systematically vary between continents, e.g. America and Europe.

Bulk density was the only soil property that exhibited (negative) correlation strength of > 0.3 to any K_h (Table 6). The underlying reasons have been discussed above. Notably, the strongest correlations were found at and very close to saturation, probably due to the detrimental effect of soil compaction on macroporosity and macropore connectivity. The more compaction, the less macroporosity remains and the higher the bulk density, which in turn decreases root growth and bioturbation (Capowiez et al., 2021; Lipiec and Hatano, 2003). The only pedo-climatic factor with relatively larger correlation strength (-0.31) with the saturated hydraulic conductivity was the bulk density (Table 6).

3.6 Effects of land use, tillage, compaction and sampling time

The average $\log_{10}$ response ratios shown in Figure 8 illustrate the effects of land use and soil management on K_h for $0 \leq h \leq 100$ mm. Note that a value of ±0.3 in the $\log_{10}$ response ratio corresponds to a factor 2. Hence, K_s for uncompacted soil was found to be approximately twice as large as for compacted soil (see Figure 8c). Arable land exhibited clearly smaller K_s than grasslands and forests, which is in line with observations made by Basche ~~&~~and DeLonge, 2019. This difference became smaller with higher tensions (Figure 8a). The large difference in K_h close to saturation was likely related to traffic compaction as well as tillage operations that were applied to the majority of the investigated arable soils, which lead to the destruction of connected biopores and hence a reduced K_s. On the other hand, tillage breaks up intact soil into individual soil aggregates, which creates, at least initially, a well-connected network of inter-aggregate pores that increase K_h in the near-saturated range (Sandin et al., 2017; Schlüter et al., 2020). This effect of tillage can explain why near-saturated K_h under conventional and reduced tillage was larger than under no-till (Figure 8b). However, in this case, even K_s was larger in the tilled fields. It is likely that K_s was reduced in the no-till treatments due to traffic compaction on the fields and a lack of soil loosening by tillage as compared to conventionally tilled treatments. Note however, that we only investigated topsoils in this study. It is not clear that how different tillage types affect K_h in the subsoil. The impact of soil compaction on K_h was clearly negative in the entire investigated range of tensions (Figure 8c), which is explained by the reduction of porosity, and especially the macroporosity during compaction (see also Figure 7b). In contrast, if the K_h measurements were carried out shortly after tillage operations, K_h was increased for all investigated tensions, especially very close to saturation (Figure 8d). This confirms that tillage initially increases K_s, but that subsequent soil consolidation preferentially disconnects the largest macropores. As a consequence, K_h at and very close to saturation is reduced more strongly than K_h for higher tensions.

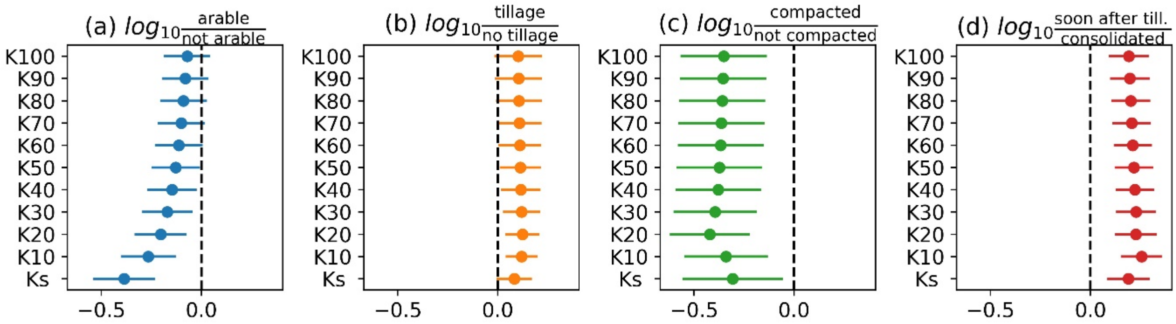

Figure 8: Weighted mean $\log_{10}$ response ratio (effect size) of K_h for from K_{100} to K_s for different management practises where the controls were 'not arable', 'no tillage', 'no compaction' and 'consolidated soil' respectively. Positive effect size means that the value of the treatment is greater than the control. Dashed line shows the "no effect" (no difference between treatment and control). Error bars represent the weighted standard error of the mean.

Figure 9 shows the results of the sensitivity analyses for the effect sizes depicted in Figure 8. The effect of land use for K_{100} turned out to be the most sensitive to the removal of studies (Figure 9a). The direction of the effect even changed after removal of six studies, indicating that higher K_{100} for arable compared to non-arable fields were not just occasional observations but occurred more frequently. More studies would be needed to properly characterise the effect of land use on K_{100}. The remaining sensitivity analyses for all the other factors showed that removal of studies did not change or destabilise the results for both K_{100} and K_s.

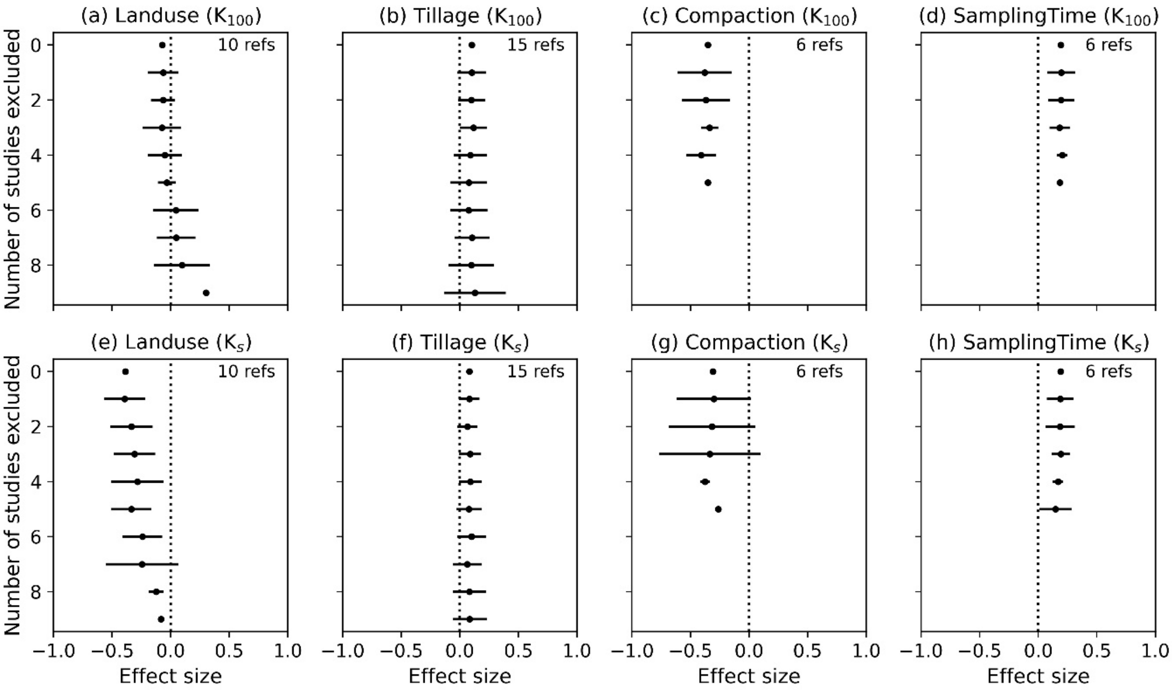

Figure 9: Sensitivity analysis of the weighted effect size of K at 100 mm tension and *K_s* for the management practice investigated using the Jackknife technique. The error bars represent the standard error.

3.7 Comparison of effect size of land use and management and sampling time with effect of climate and soil properties

Effect sizes could only be computed for land use and management, compaction as well as sampling time. It is therefore difficult to relate the impact of these factors to the ones of measurement method, climate variables and soil properties. Comparisons between figures 6, 7 and 10, on the one hand, with Figure 8 provide some insight. Land use and management related effects and sampling time (Figure 8) seem to have a similar effect on K_h as soil properties (Figure 7) and measurement method (Figure 6). Climate variables seem to have a larger impact on K_h at the dry end of the investigated tension range, but a smaller one close to saturation (Figure 10).

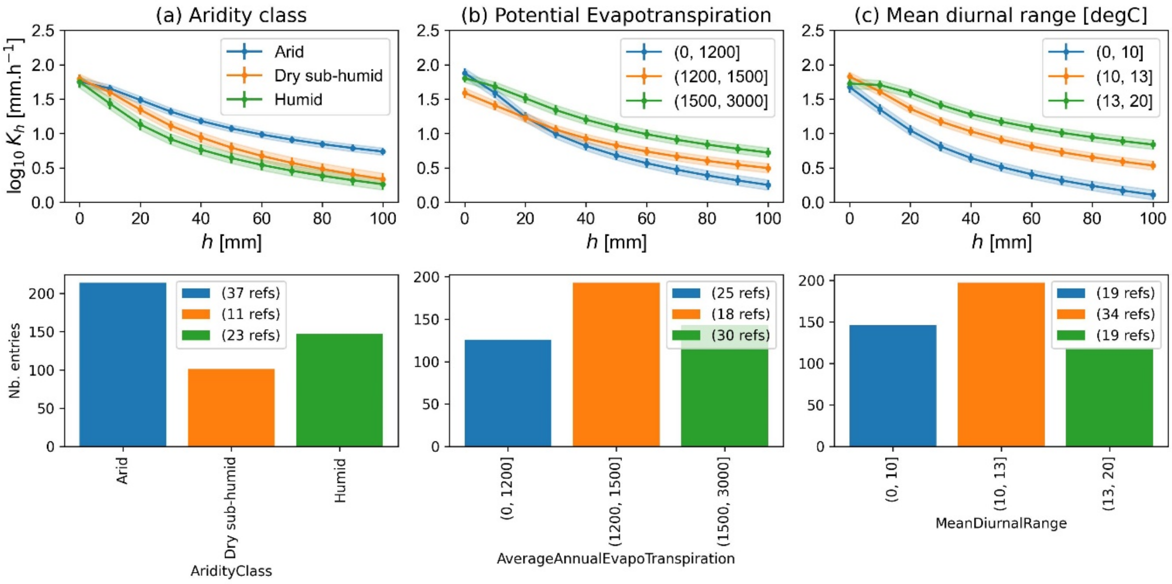

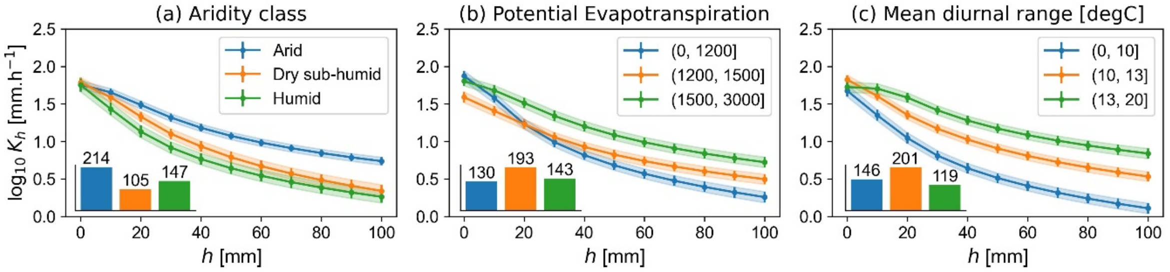

Figure 10: Evolution of weighted mean K_h as a function of applied tension for (a) aridity class, (b) potential annual evapotranspiration and (c) mean annual diurnal temperature range. The shaded areas and the error bars represent the weighted standard error of the mean.

4 Conclusions

Our results suggest that climate change will influence soil hydraulic properties near saturation. This may complicate model predictions of water balance in a future climate, particularly the risks of surface runoff, soil erosion and waterlogging. Climatic factors are more strongly correlated to near-saturated hydraulic conductivities than soil texture, bulk density and organic carbon content. At and very close to soil saturation, the correlations between hydraulic conductivity and climate variables vanished, indicating a change in flow paths. Instead, the soil bulk density showed the largest correlation, in line with the fact that more compact soils tend to lack a well-connected macropore system. Hypotheses as to why climate variables are correlated with the hydraulic conductivity were discussed, but these need to be further investigated. Most probably, the impacts of climate are linked to macropore networks associated with biological activity, pedogenesis, and land use. Only a few land use and soil management related factors could be investigated in our study. They were all found to significantly influence K_h, with effect sizes similar to those of soil properties like texture and organic carbon content. Also, experimenter bias as introduced by choice of measurement time relative to soil tillage, experimental design or data evaluation appeared to be as important for the saturated and near-saturated hydraulic conductivity as soil texture or bulk density. There is a need for better documentation and accessibility of measurement data and associated meta-data, as has already been suggested by others (McBratney et al., 2011; Basche ~~&~~and DeLonge, 2019).

5 Appendix A

5.1 Data query details

Table A1: Query strings, search engines, number of result pages that were processed and dates of the search for finding new data for OTIM

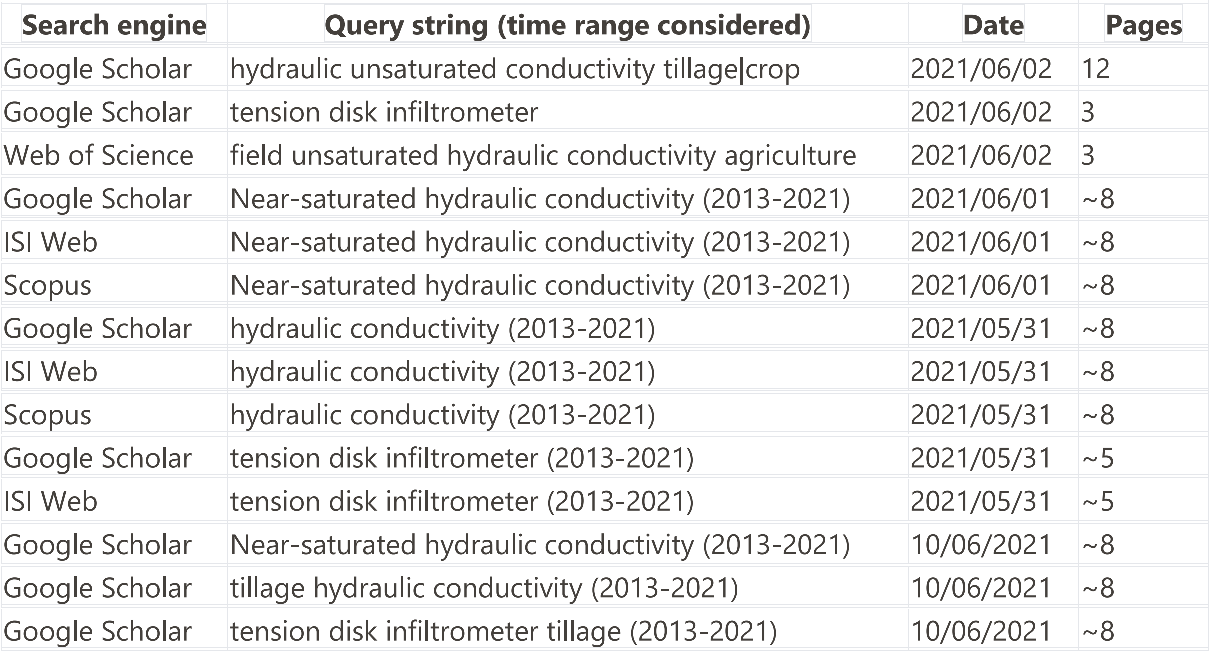

Search engine	Query string (time range considered)	Date	Pages
Google Scholar	hydraulic unsaturated conductivity tillage|crop	2021/06/02	12
Google Scholar	tension disk infiltrometer	2021/06/02	3
Web of Science	field unsaturated hydraulic conductivity agriculture	2021/06/02	3
Google Scholar	Near-saturated hydraulic conductivity (2013-2021)	2021/06/01	~8
ISI Web	Near-saturated hydraulic conductivity (2013-2021)	2021/06/01	~8
Scopus	Near-saturated hydraulic conductivity (2013-2021)	2021/06/01	~8
Google Scholar	hydraulic conductivity (2013-2021)	2021/05/31	~8
ISI Web	hydraulic conductivity (2013-2021)	2021/05/31	~8
Scopus	hydraulic conductivity (2013-2021)	2021/05/31	~8
Google Scholar	tension disk infiltrometer (2013-2021)	2021/05/31	~5
ISI Web	tension disk infiltrometer (2013-2021)	2021/05/31	~5
Google Scholar	Near-saturated hydraulic conductivity (2013-2021)	10/06/2021	~8
Google Scholar	tillage hydraulic conductivity (2013-2021)	10/06/2021	~8
Google Scholar	tension disk infiltrometer tillage (2013-2021)	10/06/2021	~8

Scopus	Near-saturated hydraulic conductivity (2013-2021)	10/06/2021	~3
Scopus	tillage hydraulic conductivity (2013-2021)	10/06/2021	~3
Scopus	tension disk infiltrometer (tillage) (2013-2021)	10/06/2021	~3
Scopus	"near-saturated" and infiltration	18/06/2021	~4
Scopus	"mini disk infiltrometer"	18/06/2021	~4
Scopus	"tension infiltrometer"	23/06/2021	~5

5.2 Data rejection

Table A2: Reasons for data rejection.

Reason	Number of publications
no access	2
not relevant	19
only one tension	61
overlap with another paper	3
no data published	32

5.3 Database organisation

OTIM is organised in nine individual tables illustrated in Table A3. The main table is named *experiments*. It contains identifiers with which all the other tables are linked. The identifiers are shown in bold font in Table A3. The *reference* table contains information on the references for each study. The *location* table lists the coordinates of the measurement sites. The tables *soilProperties*, *soilManagement* and *climate* store data as implied by their names. The *method* table gives details on the specifications of the tension-disk infiltrometer and the method to calculate hydraulic conductivity from the infiltration rate. The *rawData* table contains the hydraulic conductivities and respective supply tensions as stated in the corresponding source publication. Note that OTIM does not contain raw data for the entries of the original version compiled for Jarvis et al., 2013. Finally, *modelFit* reports K_h for $0 \le h \le 100$ mm as described above. For more details, the reader is directed to the ‘description’ tab of the database (not shown in Table A3) where the meanings and units of each column are explained.

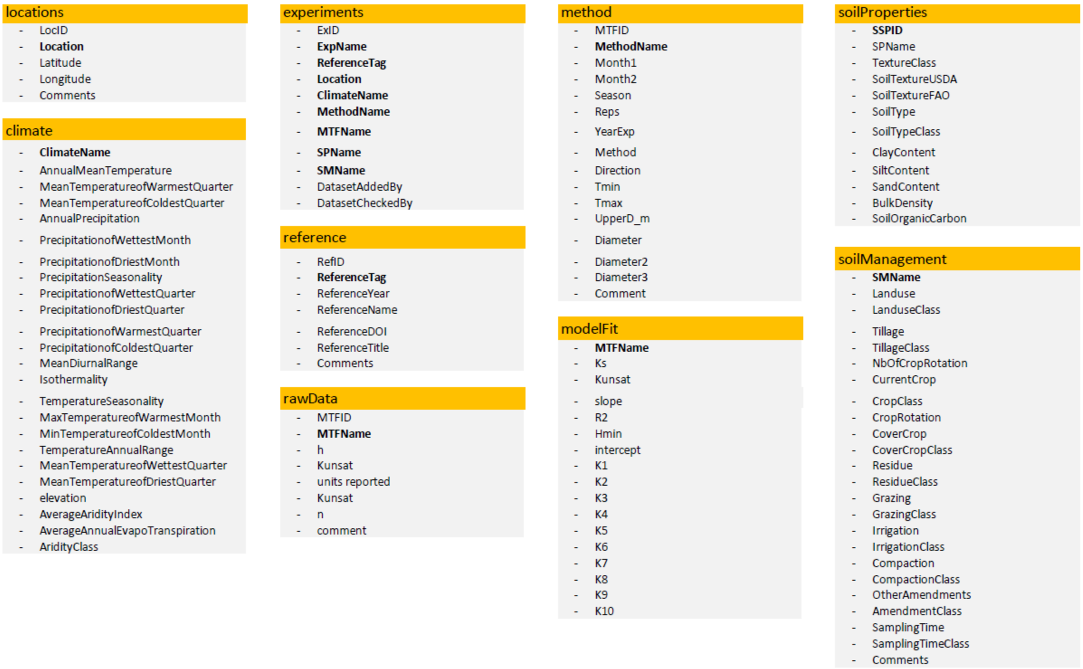

locations
- LocID
- **Location**
- Latitude
- Longitude
- Comments

climate
- **ClimateName**
- AnnualMeanTemperature
- MeanTemperatureofWarmestQuarter
- MeanTemperatureofColdestQuarter
- AnnualPrecipitation
- PrecipitationofWettestMonth
- PrecipitationofDriestMonth
- PrecipitationSeasonality
- PrecipitationofWettestQuarter
- PrecipitationofDriestQuarter
- PrecipitationofWarmestQuarter
- PrecipitationofColdestQuarter
- MeanDiurnalRange
- Isothermality
- TemperatureSeasonality
- MaxTemperatureofWarmestMonth
- MinTemperatureofColdestMonth
- TemperatureAnnualRange
- MeanTemperatureofWettestQuarter
- MeanTemperatureofDriestQuarter
- elevation
- AverageAridityIndex
- AverageAnnualEvapoTranspiration
- AridityClass

experiments
- ExID
- **ExpName**
- **ReferenceTag**
- **Location**
- **ClimateName**
- **MethodName**
- **MTFName**
- **SPName**
- **SMName**
- DatasetAddedBy
- DatasetCheckedBy

reference
- RefID
- **ReferenceTag**
- ReferenceYear
- ReferenceName
- ReferenceDOI
- ReferenceTitle
- Comments

rawData
- MTFID
- **MTFName**
- h
- Kunsat
- units reported
- Kunsat
- n
- comment

method
- MTFID
- **MethodName**
- Month1
- Month2
- Season
- Reps
- YearExp
- Method
- Direction
- Tmin
- Tmax
- UpperD_m
- Diameter
- Diameter2
- Diameter3
- Comment

modelFit
- **MTFName**
- Ks
- Kunsat
- slope
- R2
- Hmin
- intercept
- K1
- K2
- K3
- K4
- K5
- K6
- K7
- K8
- K9
- K10

soilProperties
- **SSPID**
- SPName
- TextureClass
- SoilTextureUSDA
- SoilTextureFAO
- SoilType
- SoilTypeClass
- ClayContent
- SiltContent
- SandContent
- BulkDensity
- SoilOrganicCarbon

soilManagement
- **SMName**
- Landuse
- LanduseClass
- Tillage
- TillageClass
- NbOfCropRotation
- CurrentCrop
- CropClass
- CropRotation
- CoverCrop
- CoverCropClass
- Residue
- ResidueClass
- Grazing
- GrazingClass
- Irrigation
- IrrigationClass
- Compaction
- CompactionClass
- OtherAmendments
- AmendmentClass
- SamplingTime
- SamplingTimeClass
- Comments

Table A3: Structure of the OTIM database with its different tables and columns. In the *soilManagement* table, the columns with the suffix "Class" denote columns in which the data reported in the source publications were summarised into classes to facilitate comparing them. For example, the reported *CurrentCrop* like wheat, rye, barley or oat was assigned the *CropClass* cereals. The rows in bold **denote unique identifiers with which the table entries are linked to the *experiments* table.**

6 Appendix B

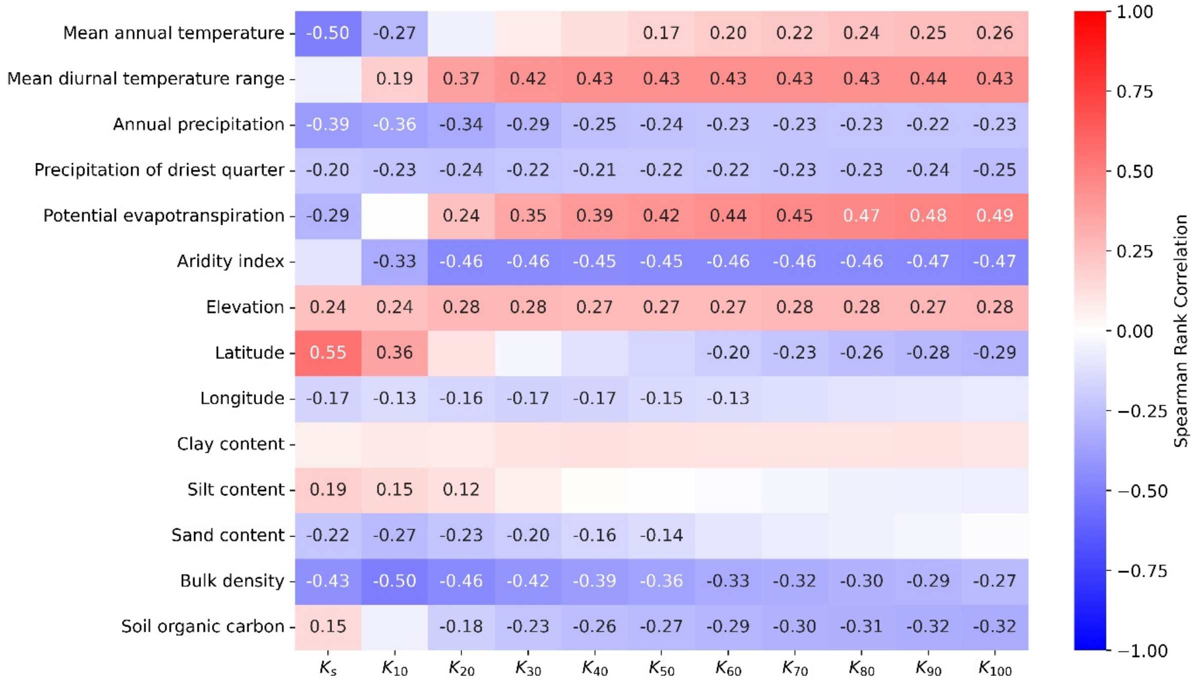

	K_s	K_{10}	K_{20}	K_{30}	K_{40}	K_{50}	K_{60}	K_{70}	K_{80}	K_{90}	K_{100}
Mean annual temperature	-0.50	-0.27				0.17	0.20	0.22	0.24	0.25	0.26
Mean diurnal temperature range		0.19	0.37	0.42	0.43	0.43	0.43	0.43	0.43	0.44	0.43
Annual precipitation	-0.39	-0.36	-0.34	-0.29	-0.25	-0.24	-0.23	-0.23	-0.23	-0.22	-0.23
Precipitation of driest quarter	-0.20	-0.23	-0.24	-0.22	-0.21	-0.22	-0.22	-0.23	-0.23	-0.24	-0.25
Potential evapotranspiration	-0.29		0.24	0.35	0.39	0.42	0.44	0.45	0.47	0.48	0.49
Aridity index		-0.33	-0.46	-0.46	-0.45	-0.45	-0.46	-0.46	-0.46	-0.47	-0.47
Elevation	0.24	0.24	0.28	0.28	0.27	0.27	0.27	0.28	0.28	0.27	0.28
Latitude	0.55	0.36					-0.20	-0.23	-0.26	-0.28	-0.29
Longitude	-0.17	-0.13	-0.16	-0.17	-0.17	-0.15	-0.13				
Clay content											
Silt content	0.19	0.15	0.12								
Sand content	-0.22	-0.27	-0.23	-0.20	-0.16	-0.14					
Bulk density	-0.43	-0.50	-0.46	-0.42	-0.39	-0.36	-0.33	-0.32	-0.30	-0.29	-0.27
Soil organic carbon	0.15		-0.18	-0.23	-0.26	-0.27	-0.29	-0.30	-0.31	-0.32	-0.32

Table B1: Weighted Spearman rank correlation coefficients between K_h at different tensions and climatic features, soil properties, land use and management factors and methodological details. In contrast to Table 6, only the 193 data entries from arable fields using a dry-to-wet sequence and the steady-state piecewise method (Reynolds and Elrick, 1991; Ankeny et al., 1991) were considered. Correlation coefficients are shown up to p-values of 0.001.

7 Code availability

All scripts used to compile this study are publically available in form of Jupyter notebooks on GitHub: https://github.com/climasoma/OTIM and https://github.com/climasoma/machine-learning.

8 Data availability

The OTIM database is available from the BONARES data repository https://tools.bonares.de/doi/datasets.

9 Author contribution

Funding acquisition: JK, SG; project administration, supervision and conceptualization: JK; meta-database collation and validation: LA, GuBl, JK; Python code development, including visualization: GuBl, JK; applying statistical analyses and writing original manuscript draft: GuBl, JK; Reviewing and editing the manuscript: JK, NJ, SG; GiBr, GuBl.

10 Competing interests

11 The authors declare that they have no conflict of interest.

12 Acknowledgements

This study was carried out in the framework of the EJP Soil ClimaSoMa project, which has received funding from the EU Horizon 2020 Research and Innovation programme under grant number 862695. We thank Lionel Alletto, Mats Larsbo, Ali Meshgi and Wim Cornelis for sharing additional details to their source publication.

13 References

Alagna, V., Bagarello, V., Di Prima, S., and Iovino, M.: Determining hydraulic properties of a loam soil by alternative infiltrometer techniques: Hydraulic Properties of a Loam Soil by Infiltrometer Techniques, Hydrol. Process., 30, 263–275, https://doi.org/10.1002/hyp.10607, 2016.

Alletto, L., Pot, V., Giuliano, S., Costes, M., Perdrieux, F., and Justes, E.: Temporal variation in soil physical properties improves the water dynamics modeling in a conventionally-tilled soil, Geoderma, 243–244, 18–28, https://doi.org/10.1016/j.geoderma.2014.12.006, 2015.

Angulo-Jaramillo, R., Vandervaere, J. P., Roulier, S., Thony, J. L., Gaudet, J. P., and Vauclin, M.: Field measurement of soil surface hydraulic properties by disc and ring infiltrometers - A review and recent developments, Soil Tillage Res., 55, 1–29, 2000.

Ankeny, M. D., Ahmed, M., Kaspar, T. C., and Horton, R.: Simple field method for determining unsaturated hydraulic conductivity, 55, 467–470, 1991.

Bagarello, V., Baiamonte, G., Castellini, M., Di Prima, S., and Iovino, M.: A comparison between the single ring pressure infiltrometer and simplified falling head techniques: COMPARING PRESSURE INFILTROMETER AND SFH TECHNIQUES, Hydrol. Process., 28, 4843–4853, https://doi.org/10.1002/hyp.9980, 2014.

Baranian Kabir, E., Bashari, H., Bassiri, M., and Mosaddeghi, M. R.: Effects of land-use/cover change on soil hydraulic properties and pore characteristics in a semi-arid region of central Iran, Soil and Tillage Research, 197, 104478, https://doi.org/10.1016/j.still.2019.104478, 2020.

Basche, A. D. and DeLonge, M. S.: Comparing infiltration rates in soils managed with conventional and alternative farming methods: A meta-analysis, 14, https://doi.org/10.1371/journal.pone.0215702, 2019.

Báťková, K., Miháliková, M., and Matula, S.: Hydraulic Properties of a Cultivated Soil in Temperate Continental Climate Determined by Mini Disk Infiltrometer, Water, 12, 843, https://doi.org/10.3390/w12030843, 2020.

Bodner, G., Scholl, P., Loiskandl, W., and Kaul, H. P.: Environmental and management influences on temporal variability of near saturated soil hydraulic properties, 204, 120–129, https://doi.org/10.1016/j.geoderma.2013.04.015, 2013.

Bottinelli, N., Menasseri-Aubry, S., Cluzeau, D., and Hallaire, V.: Response of soil structure and hydraulic conductivity to reduced tillage and animal manure in a temperate loamy soil, Soil Use Manage, 29, 401–409, https://doi.org/10.1111/sum.12049, 2013.

Bouma, J.: Using soil survey data for quantitative land evaluation, 9, 177–213, 1989.

Capowiez, Y., Sammartino, S., Keller, T., and Bottinelli, N.: Decreased burrowing activity of endogeic earthworms and effects on water infiltration in response to an increase in soil bulk density, Pedobiologia, 85-86, 150728, 2021.

Costa, J. L., Aparicio, V., and Cerdà, A.: Soil physical quality changes under different management systems after 10 years in the Argentine humid pampa, Solid Earth, 6, 361–371, https://doi.org/10.5194/se-6-361-2015, 2015.

De Boever, M., Gabriels, D., Ouessar, M., and Cornelis, W.: Influence of Acacia Trees on Near-Surface Soil Hydraulic Properties in Arid Tunisia, Land Degrad. Develop., 27, 1805–1812, https://doi.org/10.1002/ldr.2302, 2016.

Etana, A., Larsbo, M., Keller, T., Arvidsson, J., Schjønning, P., Forkman, J., and Jarvis, N.: Persistent subsoil compaction and its effects on preferential flow patterns in a loamy till soil, Geoderma, 192, 430–436, https://doi.org/10.1016/j.geoderma.2012.08.015, 2013.

Fashi, F. H., Gorji, M., and Sharifi, F.: THE USE OF SOIL HYDRAULIC PROPERTIES AS INDICATORS FOR ASSESSING THE IMPACT OF MANAGEMENT PRACTICES UNDER SEMI-ARID CLIMATES, Environ. Eng. Manag. J., 18, 1057–1066, https://doi.org/10.30638/eemj.2019.102, 2019.

Fasinmirin, J. T., Olorunfemi, I. E., and Olakuleyin, F.: Strength and hydraulics characteristics variations within a tropical Alfisol in Southwestern Nigeria under different land use management, Soil and Tillage Research, 182, 45–56, https://doi.org/10.1016/j.still.2018.04.017, 2018.

Greenwood: Land use and tillage effects on soil saturated hydraulic conductivity: Does infiltration method matter?, Master Thesis, Lincoln University, New-Zeeland, 2017.

Fick, S. E. and Hijmans, R. J.: WorldClim 2: new 1-km spatial resolution climate surfaces for global land areas, 37, 4302–4315, https://doi.org/10.1002/joc.5086, 2017.

Gupta, S., Hengl, T., Lehmann, P., Bonetti, S., and Or, D.: SoilKsatDB: global database of soil saturated hydraulic conductivity measurements for geoscience applications, 13, 1593–1612, https://doi.org/10.5194/essd-13-1593-2021, 2021a.

Gupta, S., Lehmann, P., Bonetti, S., Papritz, A., and Or, D.: Global Prediction of Soil Saturated Hydraulic Conductivity Using Random Forest in a Covariate-Based GeoTransfer Function (CoGTF) Framework, 13, e2020MS002242, https://doi.org/10.1029/2020MS002242, 2021b.

Hallam, J., Berdeni, D., Grayson, R., Guest, E. J., Holden, J., Lappage, M. G., Prendergast-Miller, M. T., Robinson, D. A., Turner, A., Leake, J. R., and Hodson, M. E.: Effect of earthworms on soil physico-hydraulic and chemical properties, herbage production, and wheat growth on arable land converted to ley, Science of The Total Environment, 713, 136491, https://doi.org/10.1016/j.scitotenv.2019.136491, 2020.

Hardie, M. A., Doyle, R. B., Cotching, W. E., Mattern, K., and Lisson, S.: Influence of antecedent soil moisture on hydraulic conductivity in a series of texture-contrast soils: INFLUENCE OF ANTECEDENT SOIL MOISTURE ON HYDRAULIC CONDUCTIVITY, Hydrol. Process., 26, 3079–3091, https://doi.org/10.1002/hyp.8325, 2012.

Hillel, D.: Introduction to Environmental Soil Physics, Academic Press, Amsterdam, 2004.

Hirmas, D. R., Giménez, D., Nemes, A., Kerry, R., Brunsell, N. A., and Wilson, C. J.: Climate-induced changes in continental-scale soil macroporosity may intensify water cycle, 561, 100–103, https://doi.org/10.1038/s41586-018-0463-x, 2018.

Holden, J., Wearing, C., Palmer, S., Jackson, B., Johnston, K., and Brown, L. E.: Fire decreases near-surface hydraulic conductivity and macropore flow in blanket peat: FIRE AND BLANKET PEAT HYDROLOGY, Hydrol. Process., 28, 2868–2876, https://doi.org/10.1002/hyp.9875, 2014.

Hyväluoma, J., Räty, M., Kaseva, J., and Keskinen, R.: Changes over time in near-saturated hydraulic conductivity of peat soil following reclamation for agriculture, 34, 237–243, https://doi.org/10.1002/hyp.13578, 2020.

Iovino, M., Castellini, M., Bagarello, V., and Giordano, G.: Using Static and Dynamic Indicators to Evaluate Soil Physical Quality in a Sicilian Area: SOIL PHYSICAL QUALITY EVALUATION BY STATIC

AND DYNAMIC INDICATORS, Land Degrad. Develop., 27, 200–210, https://doi.org/10.1002/ldr.2263, 2016.

IUSS Working Group WRB: World Reference Base for Soil Resources 2014, Update 2015. International Soil Classification System for Naming Soils and Creating Legends for Soil Maps., FAO, Rome, 2015.

Jarvis, N., Koestel, J., Messing, I., Moeys, J., and Lindahl, A.: Influence of soil, land use and climatic factors on the hydraulic conductivity of soil, 17, 5185–5195, https://doi.org/10.5194/hess-17-5185-2013, 2013.

Jorda, H., Bechtold, M., Jarvis, N., and Koestel, J.: Using boosted regression trees to explore key factors controlling saturated and near-saturated hydraulic conductivity, 66, 744–756, https://doi.org/10.1111/ejss.12249, 2015.

Kelishadi, H., Mosaddeghi, M. R., Hajabbasi, M. A., and Ayoubi, S.: Near-saturated soil hydraulic properties as influenced by land use management systems in Koohrang region of central Zagros, Iran, Geoderma, 213, 426–434, https://doi.org/10.1016/j.geoderma.2013.08.008, 2014.

Keskinen, R., Räty, M., Kaseva, J., and Hyväluoma, J.: Variations in near-saturated hydraulic conductivity of arable mineral topsoils in south-western and central-eastern Finland, AFSci, 28, https://doi.org/10.23986/afsci.79329, 2019.

Khetdan, C., Chittamart, N., Tawornpruek, S., Kongkaew, T., Onsamrarn, W., and Garré, S.: Influence of rock fragments on hydraulic properties of Ultisols in Ratchaburi Province, Thailand, Geoderma Regional, 10, 21–28, https://doi.org/10.1016/j.geodrs.2017.04.001, 2017.

Klute, A. and Dirksen, C.: Hydraulic conductivity and diffusivity: Laboratory measurements, in: Methods of soil analysis, Part 1, vol. 1, edited by: Klute, A., Soil Science Society of America, Inc., Madison, Wisconsin, USA, 687–734, 1986.

Koestel, J., Dathe, A., Skaggs, T. H., Klakegg, O., Ahmad, M. A., Babko, M., Giménez, D., Farkas, C., Nemes, A., and Jarvis, N.: Estimating the Permeability of Naturally Structured Soil From Percolation

Theory and Pore Space Characteristics Imaged by X-Ray, Water Resources Research, 54, 9255-9263, 2018.

Larsbo, M., Koestel, J., and Jarvis, N.: Relations between macropore network characteristics and the degree of preferential solute transport, 18, 5255–5269, https://doi.org/10.5194/hess-18-5255-2014, 2014.

Larsbo, M., Sandin, M., Jarvis, N., Etana, A., and Kreuger, J.: Surface Runoff of Pesticides from a Clay Loam Field in Sweden, J. Environ. Qual., 45, 1367–1374, https://doi.org/10.2134/jeq2015.10.0528, 2016a.

Larsbo, M., Koestel, J., Kätterer, T., and Jarvis, N.: Preferential transport in macropores is reduced by soil organic carbon, Vadose Zone Journal, 15, 2016b.

Lipiec, J. and Hatano, R.: Quantification of compaction effects on soil physical properties and crop growth, Geoderma, 116, 107-136, 2003.

Logsdon, S. D. and Jaynes, D. B.: Methodology for Determining Hydraulic Conductivity with Tension Infiltrometers, 57, 1426–1431, https://doi.org/10.2136/sssaj1993.03615995005700060005x, 1993.

Lopes, V. S., Cardoso, I. M., Fernandes, O. R., Rocha, G. C., Simas, F. N. B., de Melo Moura, W., Santana, F. C., Veloso, G. V., and da Luz, J. M. R.: The establishment of a secondary forest in a degraded pasture to improve hydraulic properties of the soil, Soil and Tillage Research, 198, 104538, https://doi.org/10.1016/j.still.2019.104538, 2020.

Lozano, L. A., Germán Soracco, C., Buda, V. S., Sarli, G. O., and Filgueira, R. R.: Stabilization of soil hydraulic properties under a long term no-till system, Rev. Bras. Ciênc. Solo, 38, 1281–1292, https://doi.org/10.1590/S0100-06832014000400024, 2014.

Lozano-Baez, S. E., Cooper, M., Frosini de Barros Ferraz, S., Ribeiro Rodrigues, R., Castellini, M., and Di Prima, S.: Assessing Water Infiltration and Soil Water Repellency in Brazilian Atlantic Forest Soils, display, 2020.

Matula, S., Miháliková, M., Lufinková, J., and Báťková, K.: The role of the initial soil water content in the determination of unsaturated soil hydraulic conductivity using a tension infiltrometer, Plant Soil Environ., 61, 515–521, https://doi.org/10.17221/527/2015-PSE, 2015.

McBratney, A. B., Minasny, B., and Tranter, G.: Necessary meta-data for pedotransfer functions, 160, 627–629, https://doi.org/10.1016/j.geoderma.2010.09.023, 2011.

Meshgi, A. and Chui, T. F. M.: Analysing tension infiltrometer data from sloped surface using two-dimensional approximation: ANALYSING TENSION INFILTROMETER DATA FROM SLOPED SURFACE, Hydrological Processes, 28, 744–752, https://doi.org/10.1002/hyp.9621, 2014.

Messing, I. and Jarvis, N. J.: Seasonal variation in field-saturated hydraulic conductivity in two swelling clay soils in Sweden, 41, 229–237, 1990.

Messing, I. ~~&~~and Jarvis, N.J.: Temporal variation in the hydraulic conductivity of a tilled clay soil as measured by tension infiltrometers. Journal of Soil Science, 44, 11-24, 1993.

Meurer, K., Barron, J., Chenu, C., Coucheney, E., Fielding, M., Hallett, P., Herrmann, A. M., Keller, T., Koestel, J., Larsbo, M., Lewan, E., Or, D., Parsons, D., Parvin, N., Taylor, A., Vereecken, H., and Jarvis, N.: A framework for modelling soil structure dynamics induced by biological activity, Glob. Change Biol., 26, 5382–5403, https://doi.org/10.1111/gcb.15289, 2020.

Miller, J. J., Beasley, B. W., Drury, C. F., Larney, F. J., Hao, X., and Chanasyk, D. S.: Influence of long-term feedlot manure amendments on soil hydraulic conductivity, water-stable aggregates, and soil thermal properties during the growing season, Can. J. Soil. Sci., 98, 421–435, https://doi.org/10.1139/cjss-2017-0061, 2018.

Morris, P.J., Davies, M.L., Baird, A.J., Balliston, N., Bourgault, M.-A., Clymo, R.S., Fewster, R.E., Furukawa, A.K., Holden, J., Kessel, E., Ketcheson, S.J., Kløve, B., Larocque, M., Marttila, H., Menberu, M.W., Moore, P.A., Price, J.S., Ronkanen, A.-K., Rosa, E., Strack, M., Surridge, B.W.J., Waddington, J.M., Whittington, P. and Wilkinson, S.L.: Saturated Hydraulic Conductivity in Northern Peats Inferred

From Other Measurements. *Water Resources Research*, **58,** https://doi.org/10.1016/e2022WR033181, 2022.

Nemes, A., Schaap, M. G., Leij, F. J., and Wosten, J. H. M.: Description of the unsaturated soil hydraulic database UNSODA version 2.0, 251, 151–162, 2001.

Pagliai, M., Vignozzi, N., and Pellegrini, S.: Soil structure and the effect of management practices, Soil & Tillage Research, 79, 131-143, 2004.

Poggio, L., de Sousa, L. M., Batjes, N. H., Heuvelink, G. B. M., Kempen, B., Ribeiro, E., and Rossiter, D.: SoilGrids 2.0: producing soil information for the globe with quantified spatial uncertainty, SOIL, 7, 217-240, 2021.

Pulido Moncada, M., Helwig Penning, L., Timm, L. C., Gabriels, D., and Cornelis, W. M.: Visual examinations and soil physical and hydraulic properties for assessing soil structural quality of soils with contrasting textures and land uses, Soil and Tillage Research, 140, 20–28, https://doi.org/10.1016/j.still.2014.02.009, 2014.

Rahbeh, M.: Characterization of preferential flow in soils near Zarqa river (Jordan) using in situ tension infiltrometer measurements, 7, e8057, https://doi.org/10.7717/peerj.8057, 2019.

Rahmati, M., Weihermüller, L., Vanderborght, J., Pachepsky, Y. A., Mao, L., Sadeghi, S. H., Moosavi, N., Kheirfam, H., Montzka, C., Van Looy, K., Toth, B., Hazbavi, Z., Al Yamani, W., Albalasmeh, A. A., Alghzawi, M. Z., Angulo-Jaramillo, R., Antonino, A. C. D., Arampatzis, G., Armindo, R. A., Asadi, H., Bamutaze, Y., Batlle-Aguilar, J., Béchet, B., Becker, F., Blöschl, G., Bohne, K., Braud, I., Castellano, C., Cerdà, A., Chalhoub, M., Cichota, R., Císlerová, M., Clothier, B., Coquet, Y., Cornelis, W., Corradini, C., Coutinho, A. P., De Oliveira, M. B., De Macedo, J. R., Durães, M. F., Emami, H., Eskandari, I., Farajnia, A., Flammini, A., Fodor, N., Gharaibeh, M., Ghavimipanah, M. H., Ghezzehei, T. A., Giertz, S., Hatzigiannakis, E. G., Horn, R., Jiménez, J. J., Jacques, D., Keesstra, S. D., Kelishadi, H., Kiani-Harchegani, M., Kouselou, M., Jha, M. K., Lassabatere, L., Li, X., Liebig, M. A., Lichner, L., López, M. V., Machiwal, D., Mallants, D., Mallmann, M. S., De Oliveira Marques, J. D., Marshall, M. R., Mertens, J., Meunier, F., Mohammadi, M. H., Mohanty, B. P., Pulido-Moncada, M., Montenegro, S., Morbidelli, R., Moret-Fernández, D., Moosavi, A. A., Mosaddeghi, M. R., Mousavi, S. B., Mozaffari, H., Nabiollahi, K., Neyshabouri, M. R., Ottoni, M. V., Ottoni Filho, T. B., Pahlavan-Rad, M. R., Panagopoulos, A., Peth, S., Peyneau, P. E., Picciafuoco, T., Poesen, J., Pulido, M., Reinert, D. J., Reinsch, S., Rezaei, M., Roberts, F. P., Robinson, D., Rodrigo-Comino, J., Rotunno Filho, O. C., Saito, T., et al.: Development and analysis of the Soil Water Infiltration Global database, 10, 1237–1263, https://doi.org/10.5194/essd-10-1237-2018, 2018.

Reynolds, W. D. and Elrick, D. E.: Determination of Hydraulic Conductivity Using a Tension Infiltrometer, 55, 633–639, https://doi.org/10.2136/sssaj1991.03615995005500030001x, 1991.

Rienzner, M. and Gandolfi, C.: Investigation of spatial and temporal variability of saturated soil hydraulic conductivity at the field-scale, Soil and Tillage Research, 135, 28–40, https://doi.org/10.1016/j.still.2013.08.012, 2014.

Sandin, M., Koestel, J., Jarvis, N., and Larsbo, M.: Post-tillage evolution of structural pore space and saturated and near-saturated hydraulic conductivity in a clay loam soil, 165, 161–168, https://doi.org/10.1016/j.still.2016.08.004, 1, 2017.

Schaap, M. G. and Leij, F. J.: Improved prediction of unsaturated hydraulic conductivity with the Mualem-van Genuchten model, Soil Science Society of America Journal, 64 (3), pp. 843 – 851, 2000.

Schaap, M. G., Leij, F. J., and van Genuchten, M. T.: ROSETTA: a computer program for estimating soil hydraulic parameters with hierarchical pedotransfer functions, Journal of Hydrology, 251, 163–176, 2001.

Schlüter, S., Albrecht, L., Schwärzel, K., and Kreiselmeier, J.: Long-term effects of conventional tillage and no-tillage on saturated and near-saturated hydraulic conductivity – Can their prediction be improved by pore metrics obtained with X-ray CT? Geoderma, 361, 2020.

Smettem, K. R. J. and Clothier, B. E.: Measuring unsaturated sorptivity and hydraulic conductivity using multiple disc permeameters, 40, 563–568, https://doi.org/10.1111/j.1365-2389.1989.tb01297.x, 1989.

Soracco, C. G., Lozano, L. A., Villarreal, R., Palancar, T. C., Collazo, D. J., Sarli, G. O., and Filgueira, R. R.: EFFECTS OF COMPACTION DUE TO MACHINERY TRAFFIC ON SOIL PORE CONFIGURATION, Rev. Bras. Ciênc. Solo, 39, 408–415, https://doi.org/10.1590/01000683rbcs20140359, 2015.

Soracco, C. G., Villarreal, R., Melani, E. M., Oderiz, J. A., Salazar, M. P., Otero, M. F., Irizar, A. B., and Lozano, L. A.: Hydraulic conductivity and pore connectivity. Effects of conventional and no-till systems determined using a simple laboratory device, Geoderma, 337, 1236–1244, https://doi.org/10.1016/j.geoderma.2018.10.045, 2019.

Tóth, B., Weynants, M., Nemes, A., Makó, A., Bilas, G., and Tóth, G.: New generation of hydraulic pedotransfer functions for Europe, 66, 226–238, https://doi.org/10.1111/ejss.12192, 2015.

Trabucco, A. and Zomer, R.: Global Aridity Index and Potential Evapotranspiration (ET0) Climate Database, https://doi.org/10.6084/m9.figshare.7504448.v3, 2019.

Van Looy, K., Bouma, J., Herbst, M., Koestel, J., Minasny, B., Mishra, U., Montzka, C., Nemes, A., Pachepsky, Y. A., Padarian, J., Schaap, M. G., Toth, B., Verhoef, A., Vanderborght, J., van der Ploeg, M. J., Weihermuller, L., Zacharias, S., Zhang, Y. G., and Vereecken, H.: Pedotransfer Functions in Earth System Science: Challenges and Perspectives, 55, 1199–1256, https://doi.org/10.1002/2017rg000581, 2017.

Vandervaere, J.-P., Vauclin, M., and Elrick, D. E.: Transient Flow from Tension Infiltrometers II. Four Methods to Determine Sorptivity and Conductivity, 64, 1272–1284, https://doi.org/10.2136/sssaj2000.6441272x, 2000.

Vereecken, H., Weynants, M., Javaux, M., Pachepsky, Y., Schaap, M. G., and Genuchten, M. T. v.: Using pedotransfer functions to estimate the van Genuchten–Mualem soil hydraulic properties: A review, Vadose Zone Journal, 9, 795-820, 2010.

Wang, L., Garré, S., De Cuypere, T., Pollet, S., Cornelis, W. unpublished data.

Wanniarachchi, D., Cheema, M., Thomas, R., Kavanagh, V., and Galagedara, L.: Impact of Soil Amendments on the Hydraulic Conductivity of Boreal Agricultural Podzols, Agriculture, 9, 133, https://doi.org/10.3390/agriculture9060133, 2019.

Weynants, M., Vereecken, H., and Javaux, M.: Revisiting Vereecken pedotransfer functions: Introducing a closed-form hydraulic model, 8, 86–95, https://doi.org/10.2136/vzj2008.0062, 2009.

Weynants, M., Montanarella, L., Toth, G., Arnoldussen, A., Anaya Romero, M., Bilas, G., Borresen, T., Cornelis, W., Daroussin, J., Feichtinger, F., Gonçalves, M., Hannam, J., Haugen, L., Hennings, V., Houskova, B., Iovino, M., Javaux, M., Keay, C., Kätterer, T., Kvaerno, S., Laktinova, T., Lamorski, K., Lilly, A., Mako, A., Matula, S., Morari, F., Nemes, A., Nyborg, Å., Patyka, N., Riley, H., Romano, N., Schindler, U., Shein, E., Slawinski, C., Strauss, P., Tóth, B., and Woesten, H.: European HYdropedological Data Inventory (EU-HYDI). EUR 26053, Publications Office of the European Union, Luxembourg (Luxembourg). JRC81129., 2013.

Whalley, W. R., Dumitru, E., and Dexter, A. R.: Biological effects of soil compaction, Soil and Tillage Research, 35, 53-68, 1995.

Wösten, J. H. M., Lilly, A., Nemes, A., and le Bas, C.: Development and use of a database of hydraulic properties of European soils, 90, 169–185, 1999.

Wösten, J. H. M., Pachepsky, Y. A., and Rawls, W. J.: Pedotransfer functions: bridging the gap between available basic soil data and missing soil hydraulic characteristics, 251, 123–150, https://doi.org/10.1016/S0022-1694(01)00464-4, 2001.

Wooding, R. A.: Steady Infiltration from a Shallow Circular Pond, Water Resources Research, 4, 1259-1273, 1968.

Yu, Z., Dong, W., Young, M. H., Li, Y., and Yang, T.: On evaluating characteristics of the solute transport in the arid vadose zone, 52, 50–62, https://doi.org/10.1111/gwat.12026, 2014.

Yusuf, K. O., Ejieji, C. J., and Baiyeri, M. R.: Determination of sorptivity, infiltration rate and hydraulic conductivity of soil using a tension infiltrometer, 10, 99–108, 2018.

Yusuf, K. O., Obalowu, R. O., Akinleye, G. T., and Adio-Yusuf, S. I.: Determination of Sorptivity, Infiltration Rate and Hydraulic Conductivity of Loamy Sand using Tension Infiltrometer and Double-Ring Infiltrometer, FUOYEJET, 5, https://doi.org/10.46792/fuoyejet.v5i2.501, 2020.

Zeng, C., Zhang, F., Wang, Q., Chen, Y., and Joswiak, D. R.: Impact of alpine meadow degradation on soil hydraulic properties over the Qinghai-Tibetan Plateau, Journal of Hydrology, 478, 148–156, https://doi.org/10.1016/j.jhydrol.2012.11.058, 2013a.

Zeng, C., Wang, Q., Zhang, F., and Zhang, J.: Temporal changes in soil hydraulic conductivity with different soil types and irrigation methods, Geoderma, 193–194, 290–299, https://doi.org/10.1016/j.geoderma.2012.10.013, 2013b.

Zhang, R.: Determination of Soil Sorptivity and Hydraulic Conductivity from the Disk Infiltrometer, 61, 1024–1030, https://doi.org/10.2136/sssaj1997.03615995006100040005x, 1997.

Zhang, Y., Zhao, W., Li, X., Jia, A., and Kang, W.: Contribution of soil macropores to water infiltration across different land use types in a desert–oasis ecoregion, Land Degrad Dev, 32, 1751–1760, https://doi.org/10.1002/ldr.3823, 2021.

Zhang, Z., Lin, L., Wang, Y., and Peng, X.: Temporal change in soil macropores measured using tension infiltrometer under different land uses and slope positions in subtropical China, J Soils Sediments, 16, 854–863, https://doi.org/10.1007/s11368-015-1295-z, 2016.

Zhang, Z. B., Zhou, H., Zhao, Q. G., Lin, H., and Peng, X.: Characteristics of cracks in two paddy soils and their impacts on preferential flow, Geoderma, 228–229, 114–121, https://doi.org/10.1016/j.geoderma.2013.07.026, 2014.

Zhang, Z.-H., Li, X.-Y., Jiang, Z.-Y., Peng, H.-Y., Li, L., and Zhao, G.-Q.: Changes in some soil properties induced by re-conversion of cropland into grassland in the semiarid steppe zone of Inner Mongolia, China, Plant Soil, 373, 89–106, https://doi.org/10.1007/s11104-013-1772-3, 2013.

Zhao, X., Wu, P., Gao, X., Tian, L., and Li, H.: Changes of soil hydraulic properties under early-stage natural vegetation recovering on the Loess Plateau of China, CATENA, 113, 386–391, https://doi.org/10.1016/j.catena.2013.08.023, 2014.

Zhou, B. B., Wang, Q. J., and Wu, X. B.: Optimal disc tension infiltrometer estimation techniques for hydraulic properties of soil under different land uses, 9, 92–98, https://doi.org/10.3965/j.ijabe.20160904.2161, 2016.

کریمییان, ن.: اثر روش‌های خاکـورزی و مدیریت بقایای گیاهی and میرزاوند., ج., موسوی, س. ع. ا., ثامنی, ع., افضلی نیا, ص برهدایت هیدرولیکی غیر اشباع خاک در تناوب گندم – ذرت, مجله پژوهش‌های حفاظت آب و خاک, 23 https://doi.org/10.22069/jwfst.2016.3190, 2016.